Title: Cold-blooded vertebrates evolved organized germinal center like structures

Authors: Yasuhiro Shibasaki[1,2]§, Sergei Afanasyev[3#], Alvaro Fernández-Montero[1#], Yang Ding[1], Shota Watanabe[2], Fumio Takizawa[1,4], Jesús Lamas[5], Francisco Fontenla[6], José Manuel Leiro[7], Aleksei Krasnov[8]‡, Pierre Boudinot[9]‡, J. Oriol Sunyer[1]*

5 **Affiliations:**

[1]Department of Pathobiology, School of Veterinary Medicine, University of Pennsylvania; Philadelphia, PA, 19104, USA.

[2]College of Bioresource Sciences, Nihon University; Kameino 1866, Fujisawa, Kanagawa, 252-0880, Japan.

10 [3]I.M.Sechenov Institute of Evolutionary Physiology and Biochemistry, Laboratory of Neurophysiology and Behavioral Pathology; Torez 44, Saint-Petersburg, 194223, Russia.

[4]Faculty of Marine Science and Technology, Fukui Prefectural University; Obama, Fukui, 917-0003, Japan.

[5]Department of Functional Biology, Institute of Aquaculture, Campus Vida, University of
15 Santiago de Compostela; Santiago de Compostela, E-15782, Spain.

[6]Department of Functional Biology, Campus Vida, University of Santiago de Compostela; Santiago de Compostela, E-15782, Spain.

[7]Laboratory of Parasitology, Department of Microbiology and Parasitology, Institute of Research on Chemical and Biological Analysis, Campus Vida, University of Santiago de Compostela;
20 Santiago de Compostela, E-15782, Spain.

[8]Nofima AS; Osloveien 1, Ås, 1433, Norway.

[9]Universite Paris-Saclay, INRAE, UVSQ, VIM; Jouy-en-Josas, 78350, France.

[#]These authors contributed equally to this work.

5 *Primary corresponding author. Email: sunyer@vet.upenn.edu (J.O.S.)

‡Equal secondary corresponding authors. Emails: pierre.boudinot@inrae.fr (P.B.)

Aleksei.Krasnov@nofima.no (A.K.)

§This author is a Japan Society for the Promotion of Science (JSPS) Overseas Research Fellow.

10

Abstract

Germinal centers (GCs) or analogous secondary lymphoid microstructures (SLMs) are thought to have evolved in endothermic species. However, ectotherms~~their ectothermic ancestors~~ can mount potent secondary antibody (Ab) responses upon infection or immunization, despite the apparent lack of SLMs in these cold-blooded vertebrates. How and where adaptive immune responses are induced in ectothermic species in the absence of GCs or analogous SLMs remains poorly understood. Here we infected a teleost fish (trout) with the parasite *Ichthyophthirius multifiliis* (Ich) and identified the formation of large aggregates of highly proliferating IgM^+ B cells and $CD4^+$ T cells, contiguous to splenic melanomacrophage centers (MMCs). Most of these MMC-associated lymphoid aggregates (M-LAs) contained numerous antigen (Ag)-specific B cells. Analysis of the IgM heavy chain CDR3 repertoire of microdissected splenic M-LAs and non M-LA areas revealed that the most frequent B cell clones induced after Ich infection were highly shared only within the M-LAs of infected animals. These M-LAs represented highly polyclonal SLMs in which Ag-specific B cell clonal expansion occurred. M-LA-associated B cells expressed high levels of activation-induced cytidine deaminase and underwent significant apoptosis, and somatic hypermutation of Igμ genes occurred prevalently in these cells. Our findings demonstrate that ectotherms evolved organized SLMs with GC-like roles. Moreover, our results also point to primordially conserved mechanisms by which M-LAs and mammalian polyclonal GCs - develop and function.

One Sentence Summary: Cold-blooded vertebrates evolved organized SLMs with GC-like functions.

Main Text:

INTRODUCTION

Immunoglobulin (Ig)-based adaptive immunity in jawed vertebrates emerged more than 500 million years ago (*1, 2*). Elasmobranchs are the oldest vertebrate group with living representatives that bear bonafide Ig's, a spleen, and B- and T-cells (*3*). The immune system has since evolved into the highly compartmentalized and exquisitely fine-tuned adaptive response seen in modern day mammals (*2, 4*), including the appearance of class-switch recombination (CSR), which first arose in the ancestors of amphibians (*5*), and organized secondary lymphoid microstructures (SLMs) such as germinal centers (GCs), that first arose in the ancestors of birds (*4, 6*). It is thought that organized SLMs evolved to maximize encounters between antigen (Ag), antigen presenting cells (APCs), and B/T lymphocytes to efficiently sustain the B cell clonal expansion and affinity maturation processes required to fine tune adaptive antibody responses. Despite of their lack of GCs and SLMs, cold-blooded species including teleost fish, can mount potent Ag-specific secondary antibody responses upon infection or immunization (*1*). How and where adaptive immune responses are induced in these species in the absence of GCs or analogous SLMs is not understood.

All ectothermic jawed vertebrates express several classes of Ig's, although the specific gene isotypes differ between groups (*1, 3*). Their Ig rearrangement machinery is largely conserved across these species, and their primary Ig repertoires are highly diversified, similar to those of birds and mammals (*3*). Titers of systemic antigen-specific Ig of jawed ectotherms, which are mainly IgM in fish or IgY in amphibians and reptiles, significantly increase upon infection or immunization (*1*). Although Ig-specific titers can increase significantly upon reinfection or boosting, antibody affinity maturation remains relatively poor (*3*). This has been connected to the lack of GCs in ectotherms, leading to the theory that selection of high affinity B cells by somatic

hypermutation (SHM) may be compromised in these animals (*3*). However, all jawed vertebrates contain genes homologous to activation-induced cytidine deaminase (AID), the enzyme that mediates both CSR and SHM (*3, 7*). AID expression has also been reported in the spleen of fish and amphibians, although its localization and expression patterns at the cellular level remain
5 poorly understood (*7, 8*). The presence of AID in these species supports the ability of their Ig genes to undergo SHM (*9, 10*).

While the induction of SLMs has never been described in fish, Ig^{+} clusters of cells have been observed in proximity to melanomacrophage (MM) centers (MMCs), which are aggregates of dark, pigmented phagocytes mainly found in the head kidney and spleen of cold-blooded
10 vertebrates (*11-14*). MMCs increase in size following infection and trap antigen (*15*), suggesting that these teleost MMCs may represent functional analogs of GCs or lymphoid follicles (*15, 16*). However, no visible tissue organization (e.g., B-T cell zones) has yet been identified in ectotherms.

In this study, we investigated whether ectothermic vertebrates have evolved lymphoid
15 microstructures analogous to GCs to support antibody responses. We identified that induction of systemic Ab responses in teleost fish occurs in primordially organized and highly polyclonal SLMs, where structurally and functionally analogous processes to those of GCs occur.

RESULTS

Infection induces IgM$^+$ B cell proliferation and aggregation adjacent to melanomacrophage centers

To identify sites of immune responses within the infected teleost spleen, we searched for EdU$^+$
5 areas which could indicate lymphocyte proliferation and expansion. Trout (*Oncorhynchus mykiss*) were infected with the parasite *Ichthyophthirius multifiliis* (Ich), which induces strong systemic IgM responses, and IgT driven mucosal responses (*17-20*). At two weeks post-reinfection we identified aggregates of dark-colored melanomacrophages that represent MMCs (fig. S1) (*15*), which were significantly larger in infected animals than non-infected controls (Fig.
10 1A-C). Cell proliferation was significantly higher in infected spleens compared to control ones (Fig. 1 A, B, D), and was mainly concentrated in areas surrounding MMCs (Fig.1E). The number of EdU$^+$ cells inside of MMCs was significantly lower in control spleens than in infected fish (Fig. 1B, E). We observed significant numbers of IgM$^+$ B cell (IgM^{hi}) aggregates in close proximity to MMCs in infected spleens (Fig. 1B, F, fig. S1B), which were not detected in control
15 fish. B cell aggregates associated with MMCs in control animals were much smaller or absent, and contained very few IgM^{hi} B cells (Fig. 1A, F, fig. S1A). In both infected and control fish, IgM$^+$ B cells outside MMC areas were for the most part IgM^{low} (Fig. 1A-B, F, fig. S1).

Furthermore, red and white pulp areas were intermingled throughout the spleen and not separated into distinct regions (fig. S1), as previously reported (*21-23*). MMCs in infected fish
20 were more frequently associated with white pulp regions, and were populated with more lymphocytic cells when compared control fish (fig. S1). Together these results indicate that the large proliferative responses observed in areas adjacent to MMCs in infected animals suggest that processes of immune activation occur in splenic tissue areas surrounding MMCs.

Large aggregates of highly proliferating IgM^+ B and $CD4^+$ T cells are induced adjacent to MMCs upon infection

To further evaluate whether MMC adjacent IgM^+ B cell aggregates represent inductive sites of immune responses, we next assessed whether $CD4^+$ T cells were also present amongst these
5 IgM^+ B cell aggregates, since organized SLMs in mammals are typically characterized by the presence of closely associated B and T cell zones (*24, 25*). To identify $CD4^+$ T cells, we generated an anti-trout CD4 polyclonal antibody (pAb) (fig. S2). We found that upon infection, a majority of MMC areas containing IgM^+ B cell aggregates were in close proximity to $CD4^+$ T cell zones (Fig. 2, A-B). In many instances, B- and T cell-like zones were clearly defined (i.e.,
10 (Fig. 2, A(i) and B(i)), while in others, boundaries between B and T cell aggregates were somewhat diffuse (fig. S3, A(i) and B(i)). We have named these organized lymphoid tissue areas (which include both the MMCs and their associated B/T cell aggregates) as MMC-associated lymphoid aggregates (M-LAs). Within M-LAs from infected fish, significantly more IgM^+ B cells were in contact with MMCs when compared to those of $CD4^+$ T cells (Fig. 2, A(i), B(i), and
15 D). M-LAs from infected fish contained more proliferating cells (Fig. 2, A(ii), B(ii)) than those of control animals (Fig. 2, C(ii) and E). Accordingly, a large percentage of IgM^+ B cells (Fig. 2, A(iii and iv), B(iii and iv), and E) and $CD4^+$ T cells (Fig. 2, A(iii and v), B(iii and v), and E) within these M-LAs were proliferating, suggesting expansion of Ag-specific B and T cells in these areas. While control fish also contained M-LAs, they were much smaller in size (Fig.
20 2C(i), and Fig. 3A), and contained far fewer proliferating T and B cells (Fig. 2, C(iii-v) and E). Together these data suggest that induction of systemic IgM responses occurs in M-LAs.

M-LAs from immunized fish contain significant numbers of Ag-specific IgM^+ B cells

The strong proliferation of IgM^+ B cells observed in M-LAs from infected fish suggested the presence of Ag-specific B cells in these tissue microstructures. To evaluate this hypothesis, we modified a reported method developed in rats (*26*) to detect antigen on B cells from tissue sections, and adapted it to our spleen cryosections (fig. S4). To detect sufficient Ag-specific B cells, we used the T-cell dependent Ag (Dinitropheny-Keyhole limpet haemocyanin [DNP-KLH]) which is known to induce strong IgM responses in rainbow trout (*27*). At two weeks post boost, high DNP-specific IgM endpoint titers (102,400-409,600) were detected in sera. Detection of DNP-PE Ag was negligible from all M-LAs or non-M-LA areas of control fish (Fig. 3A, D). DNP-KLH-induced M-LAs (Fig. 3B) contained large aggregates of IgM^+ B cells in close proximity to both MMCs and $CD4^+$ T cell zones (Fig. 3, B-C). In immunized spleens, DNP-PE Ag co-localized with M-LA-associated IgM^+ B cells (M-LA B cells) for the most part, which represented 98.3 ± 1.2% of all the Ag-positive cells (Fig. 3, B-C). Moreover, a large proportion of the M-LA B cells were Ag-positive, while Ag signal was residual on $CD4^+$ T cells and negligible in non M-LA areas of the same fish (Fig. 3, B-D). In immunized fish, a large percentage of M-LAs (59.8 ± 8.5%) contained significant proportions of Ag-specific B cells (Fig. 3B, E), while tissue areas from MMCs not associated with B and T cell aggregates (Fig. 3B, yellow circles) were devoid of Ag binding in these fish. Flow cytometric analysis confirmed the increases of splenic antigen-specific IgM^+ B cells in the spleen of immunized fish, while negligible Ag binding was detected on $CD4^+$ T cells (fig. S5A, C), or in IgM^+ and $CD4^+$ T cells from control fish (fig. S5, B-C). Overall these results support the notion that antigen-specific clonal B cell expansion occurs within M-LAs.

CDR3 repertoire analysis demonstrates that M-LAs from infected fish share a large proportion of their most frequent CDR3s

We next determined whether the proliferating Ag-specific IgM^{+} B cells in M-LAs from infected fish were undergoing clonal expansion and selection. To this end, we analyzed the IgM heavy chain (IgHμ) repertoire of Ich infected or control fish by sequencing the expressed IgHμ CDR3 region of laser capture microdissected M-LAs and non M-LA areas (fig. S6).

5 We first compared the degree of overlap or sharing of the CDR3 sequences obtained from M-LA and non M-LA areas of the spleen of immunized animals. To this end, we determined to what extent the most frequent CDR3s (Top1000 and Top50 CDR3s) obtained from each M-LA and non M-LA area were present in other M-LA or non M-LA areas of the same spleen (Fig. 4A). A large proportion (~248-436) of the Top1000 CDR3 sequences from each M-LA were also
10 detected in other M-LAs in a representative fish (Fig. 4A(i)) (e.g. 330 of the Top1000 CDR3s found in M-LA1 were also identified in M-LA2 (Fig. 4A(ii)). Conversely, a significantly lower proportion (~91-247) of these Top1000 CDR3s found in M-LAs was present in non M-LA areas, and an even lower fraction (~28-169) of the Top1000 CDR3s from each of the non M-LA areas was detected in the other non M-LA regions (Fig. 4A(i)). This pattern of CDR3 sharing was also
15 observed when analyzing the Top50 CDR3s of M-LA and non M-LA areas of the same fish spleen (Fig. 4A(i)). As an example of this CDR3 overlap, we found that 32 of the Top50 CDR3s found in M-LA1 were also identified in M-LA2 (Fig. 4A(ii)). To evaluate whether the high sharing of the most frequent CDR3s among the M-LAs of infected fish was statistically significant, we computed the shared proportions of the Top50 CDR3s among all M-LAs and non
20 M-LA areas from several infected and control fish (Fig. 4B). The degree of sharing of the Top50 CDR3s among the different M-LA and non M-LA areas reached its highest level (~46%) only when comparing pairwise all M-LAs from infected fish (i.e., Top50 CDR3s from M-LAs found in all CDR3s from M-LAs [pointed by the magenta arrow in Y axis of Fig. 4B]), in line with our

observation from a representative fish (Fig. 4A). This finding indicates that the highest degree of co-occurrence (or sharing) of the most frequent CDR3s induced upon infection was observed mainly in the M-LAs of each of these animals. An appreciable degree of sharing of the most frequent CDR3s was also observed also among M-LAs from control fish (Fig. 4B, green arrow)
5 although it was more infrequent than that of M-LAs from infected fish. This CDR3 overlap in M-LAs from control fish may reflect a residual response due to prior exposure of these fish to other immunogens.

We next evaluated whether the overlap of the top frequent CDR3s induced in the response was widespread across M-LAs throughout the same spleen. We selected the Top50 CDR3s of each of
10 the three M-LAs analyzed from the spleen of each infected or control fish, and calculated which proportion of these CDR3s were concurrently detected in all three M-LAs (Fig. 4C). The same calculation was also done for the Top50 CDR3 sets of each three non M-LA areas analyzed from the same fish. The mean proportion of the Top50 CDR3s common to all three analyzed M-LAs was increased in the infected group and was over ten-fold higher than the proportion of Top50
15 CDR3s common to all non M-LA areas (Fig 4C (i)). As an example of this CDR3 overlap among M-LAs of infected fish, we found that a total of 7 Top50 CDR3s (i.e., ~14% of these CDR3s) were shared by all three M-LAs of the same spleen from a representative infected fish (Fig. 4C(ii)). In conclusion, this significant sharing of the most frequent CDR3 sets among all M-LAs of the same spleen in each of the infected fish, suggests an expansion of these Ag-specific B cell
20 clones.

We next assessed to which degree the shared Top50 CDR3s found in all M-LAs were expressed across individual M-LAs and non M-LA areas from the spleen of a representative infected and control fish. We found that only one Top50 CDR3 was shared by all three analyzed M-LAs from

the spleen of a representative control animal (Fig. 4D(i)). In contrast, we found ten Top50 CDR3s present in all three analyzed M-LAs from the infected spleen (Fig. 4D(ii)). Furthermore, 7 out of 10 of these CDR3s were expressed at a frequency higher than 0.5% in all 3 M-LAs. None of these CDR3s were concurrently detected in the non M-LA areas of the same spleen. For example, the number of illumina sequence reads detected for CDR3#1 in M-LA1 (3799 reads) represents 2.6% of all the CDR3 reads (143703 reads) sequenced from M-LA1 of that representative fish (Fig. 4D(iii)), whereas CDR3#1 reads were not detected in any of the non M-LA areas of the same fish (Fig. 4D(ii)). Overall, these data suggest that highly expressed CDR3s correspond to Ag-specific B cell clonal expansion.

To support further the idea that the most abundant CDR3s induced in the M-LAs of infected fish are specific for the antigen (*i.e.*, Ich parasite), we evaluated whether a different antigen (DNP-KLH) could induce a completely different set of CDR3 sequences. The overlap in CDR3s obtained by the two different antigen exposures was marginal (Fig. 4E). No public responses (public CDR3 expansions) to Ich were detected in the M-LA or non M-LA areas of infected animals.

Overall our results indicate that a large fraction of the most frequent CDR3s from a given M-LA of an infected fish are shared and highly expressed in all M-LAs from the same fish. This IgHμ repertoire convergence only in M-LAs of infected fish points to the induction of Ag-specific B-cell expansions upon infection.

M-LA B cells express high levels of AID and undergo significant apoptosis

Given that M-LAs in infected fish contain clonally expanded Ag-specific B cells, we next investigated AID expression, which in mammals is expressed at its highest levels in GC B cells (*25, 28*). AID expression was clearly detectable and mainly localized in M-LAs (outlined in

white) of infected fish (Fig. 5B) where ~43±4% of M-LAs contained significant numbers of AID$^+$ cells (Fig. 5C). In contrast, AID expression was minimal in the M-LAs or non M-LA areas of control fish (Fig. 5A, C). A large percentage of M-LA B cells were AID$^+$ (Fig. 5E)**,** while a low proportion of non M-LA B cells in the same fish expressed AID (Fig. 5B, D).

In mammals AID is responsible for a large percentage of apoptosis in GC B cells, particularly in the dark zone (DZ) (*25, 28*), and is considered a fundamental mechanism to counteract the large degree of B cell proliferation within GCs (*25, 28*). Given the high rate of M-LA B cell proliferation in infected fish (Fig. 2E) combined with their expression of AID (Fig. 5B, D), we next determined whether a proportion of M-LA B cells were apoptotic. Activated caspase 3 staining was used to detect apoptosis, which was mainly detected within M-LA B cells of infected animals (Fig. 6, A-D). ~75% of M-LAs from infected fish contained casp3$^+$ B cells, compared to only ~34% of M-LAs from control fish (Fig. 6E). Casp3 in B cells displayed a typical punctuated staining (Fig. 6, A-B), as previously reported (*29*). The highest proportion of casp3$^+$ B cells was found within M-LAs of infected fish, which contained more than double of that found in control animals (Fig. 6D), whereas the proportion of casp3$^+$ B cells in non M-LA areas was small in both control and infected fish (Fig. 6D). In addition, the proportion of casp3$^+$ CD4$^+$ T cells was minimal both in M-LA and non M-LA areas of both infected and control fish (Fig. 6, A-D). These findings suggest that AID expression in the spleen of infected fish is concentrated on M-LA B cells, and that apoptosis of these cells is a mechanism to offset their high rates of proliferation in these species.

Somatic hypermutation occurs prevalently in M-LA-associated B cells

SHM of Ig genes in warm-blooded vertebrates is known to occur mainly in GC B cells (*25*). We next explored whether AID expression in M-LA B cells was associated with the occurrence of

SHM of IgHμ V genes in these cells (Fig. 7). To look for evidence of SHM, we assessed IgHμ V sequence variation among sequences expressed by B cells belonging to the same clonal sets. Variation within sequences was measured by evaluating the sequence changes within the CDR1-FR2-CDR2-FR3 region of their V domain. Thereafter, the variation rate in a clonal set was computed after comparison with the most frequent sequence of that specific clonal set (Fig 7A). Since CDR3 repertoire analysis revealed that the most frequent clonal sets were shared among M-LAs of a spleen of an immunized fish (Fig. 4), we reasoned that evidence of SHM could be most likely detected when comparing sequence variation within clonal sets shared by splenic M-LAs from these fish. To this end, sequence variation was analyzed in clonal sets shared among M-LA and non M-LA areas of the same spleen from immunized and control fish respectively. Sequence variation was highest in the shared clonal sets of M-LAs from both control and immunized fish (Fig. 7B). In comparison to M-LAs, sequence variation in clonal sets from non M-LA areas was significantly lower than that of M-LAs, and we did not find significant differences when comparing sequence variation of shared versus non-shared clonal sets in these areas (Fig. 7B). While the rate of variation was roughly similar within clonal sets shared across M-LAs from control and infected fish, the proportion of shared B cell clones was much higher in M-LAs from infected fish, as seen in Fig. 4. Accordingly, hypermutated B cell clones were found more abundantly in M-LAs from infected fish than M-LAs from control animals. As an example of sequence variation in a clonal set shared by three different M-LAs of an infected fish, we depict a dominant clonal set tree (Fig. 7C) and show multiple sequence alignments of a subcluster of the tree displaying accumulation of mutations (Fig. 7D). The sequence alignments show significant amount of base non-silent mutations in several clonal set variants (b-h sequences in upper panel of Fig. 7D) which lead to changes in amino acid composition of these

variants (lower panel of Fig. 7D). Overall, these data indicate that upon infection, SHM of Igμ genes occur for the most part in M-LA B cells and is prevalent in Ig clonal sets specifically shared by the different splenic M-LAs of the same individual.

5

DISCUSSION

In this study we have addressed how and where adaptive immune responses are induced in species where GCs or analogous SLMs have not been described. It is well accepted that the spleen of cold-blooded jawed vertebrates represents a secondary lymphoid organ in which B and T cell responses have been shown to occur, and thus, it is believed that secondary immune responses are induced in this organ (*3*). However, whether B-T cell interactions leading to such responses occur stochastically in random areas of the spleen or in a specific splenic microenvironment, is a question that has remained elusive for decades. Supporting the later scenario, our results indicate that induction of systemic Ab responses in teleost fish occur in primordially organized and highly polyclonal SLMs that are structurally and functionally analogous to GCs. More specifically, our unbiased strategy to identify inductive sites of the immune response in the fish spleen led to the discovery of SLMs which we named as M-LAs. These M-LAs are inducible tissue microstructures comprised of MMCs and their associated B and T cell aggregates. Upon infection or immunization, M-LA-associated B and T cells proliferate, while M-LA B cells express high levels of activation-induced cytidine deaminase and undergo significant apoptosis. Critically, antigen-specific B cell clonal expansion and SHM processes mostly occur in the induced M-LAs and not in the surrounding non-M-LA areas.

While there are a number of structural and functional similarities between M-LAs and GCs, there exist also significant differences, most critically: **1)** T cell zones are inducible only in M-LAs; **2)** M-LAs lack the light and dark zones found in GCs; **3)** GCs are localized within highly organized lymphoid areas (i.e., lymph nodes and tertiary lymphoid organs), but M-LAs are not; **4)** GCs contain FDCs which retain antigen while in M-LAs this role might be played by MMCs. We cannot rule out that some of above stated differences between M-LAs and GCs may reflect the

current limitations imposed by our animal model, including the absence of antibody reagents specific for fish immune molecules that can distinguish other key leukocyte markers (i.e., macrophages) and subsets of B cells in various states of differentiation (i.e., plasmablast, plama cells, memory B cells). From an evolutionary perspective, we propose that the most primordial SLMs primarily evolved to promote processes of antigen-specific B cell clonal expansion which in turn led to the generation of highly amplified Ag-specific Ab responses. In early jawed vertebrates these SLMs arose as open, polyclonal, and rudimentarily organized SLMs (analogous to M-LAs). Due to their primitive organization (and consistent with the low affinity antibody responses reported for cold-blooded species (*17*)) these primeval SLMs or M-LA-like structures would contain mostly low affinity B cell clones due to their inability to select high affinity ones. Over evolutionary time, and with the acquisition of novel immunological innovations (i.e., FDCs, dark/light GC zones, more efficient AID, lymph nodes), SLMs of early endotherms evolved to fine tune Ab responses through their new capacity to select high affinity B cell clones, which led to vast improvements in the affinity of the resulting Ab responses. Further evolution of these more highly organized SLMs in mammals probably led to the emergence of GCs with two main types of clonal composition, the newly identified polyclonal GCs (*30*) and the well-known homogeneous GCs composed of only a few selected and expanded high affinity B cell clones. It is possible that polyclonal GCs and M-LAs have derived from primordial M-LA-like structures that emerged in the common ancestors of teleosts and mammals. Alternatively, polyclonal GCs and M-LAs arose independently through convergent evolutionary processes.

The induced B and T cell aggregates in these M-LAs showed different degrees of organization. It is possible that the less organized B-T cell zones in some of these M-LAs represent

intermediate stages of M-LA maturation. While control fish also contained M-LAs, they were much smaller in size and clear B and T cell zones were for the most part absent. In control fish, these small M-LAs could be aging M-LAs induced by previous antigenic exposure, or M-LAs in the process of shutting down, similar to what has been described for mammalian GCs (*31*).
5 Alternatively, they may represent active M-LAs induced by low concentrations of environmental Ag, auto-Ag, or Ag derived from microbiota translocating from mucosal areas. In that regard, it has been shown that gram-negative microbiota from the gut of humans and mice continuously translocate at low levels into the bloodstream thereby inducing significant specific systemic antibody responses (*32*). Interestingly, we have previously reported that a large proportion of the
10 trout microbiota are coated by IgM (*33*). Thus, microbiota-specific B cells might be induced in M-LAs possibly by translocated microbiota. Further work will need to evaluate the aforementioned possibilities.

While the induction of M-LAs or similar structures has never been described in fish, it has been proposed that fish MMCs could represent functional analogs of GCs (*15, 16*), in part because of
15 their reported role in trapping antigen. Accordingly, melanomacrophages from these centers might play a role analogous to that of GC-associated follicular dendritic cells (FDCs), and thus, MMCs could function in the selection of cognate B cells upon antigenic challenge. In support of this hypothesis, we saw large numbers of M-LA B cells, but not $CD4^+$ T cells, in contact to MMCs. Selection of Ag-specific B cells could lead to clonal expansion of these selected B cell
20 clones, as shown in this study. Upon infection, expansion of B cells in some teleosts has also been observed in mucosal lymphoid tissues lacking MMCs (*19, 34, 35*). Thus, the possibility exists that these B cell-containing areas without MMCs may also represent inductive sites of the immune response. For example, the presence of a novel organized nasopharynx-associated

lymphoid tissue (O-NALT) in teleosts was recently identified (*35*). Upon viral infection, IgM$^+$ B cell numbers increased in the O-NALT, and this was accompanied by upregulation of *aicda* and *cxcr4* transcripts in the same tissue as well as in the tip of the NALT, which is considered a non-organized lymphoid tissue. The authors concluded that O-NALT expresses molecular markers that resemble mammalian GC reactions, and further work is warranted to evaluate whether O-NALT and other teleost lymphoid regions devoid of MMCs may functionally behave as GC analogs. In contrast to teleosts, some cold-blooded species contain B cell follicles, and those regions could represent tissue areas where adaptive immune responses are induced. For instance, sharks have previously been shown to contain B cell follicles (*3*), and a recent study reported that nurse shark B cell follicles constitute organized B cell selection sites where immune responses appear to be induced (*36*). B cell follicles have also been described in the adult *Xenopus* spleen, and while they are not present in all amphibian species (*3*), they appear to contain most of the celular and molecular machinery required for the induction of adaptive immune responses (*37*).

The high proliferative rate of M-LA B cells upon infection or immunization led to the hypothesis that B cell proliferation was induced in an Ag-dependent manner. In support, we found that a very high proportion of M-LAs from these fish contained significant amounts of Ag-specific B cells which suggested the common presence or "sharing" of Ag-specific B cell clones among the induced M-LAs of the same spleen. Reinforcing this notion, IgHμ CDR3 repertoire analysis showed that large numbers of the most frequent CDR3s induced upon infection were extensively shared between M-LAs from the same spleen, and most of these shared CDR3s were highly expressed in all analyzed M-LAs from the same individual. Critically, the degree of sharing of the most frequent CDR3s in non M-LA areas from the same infected fish was much lower than that found within M-LAs, thus implying that M-LAs were the microanatomic sites were

processes of B cell clonal expansion were taking place, congruent also with the strong proliferative IgM^+ B cell responses we observed in these M-LAs. The CDR3 repertoire data herein reported indicate that M-LAs are highly polyclonal structures and that sharing of the most frequent CDR3s among M-LAs of antigen-stimulated animals is an important feature of fish M-LAs.

The CDR3 repertoire data herein reported support the notion that fish M-LAs are highly polyclonal structures where processes of antigen-specific B cell clonal expansion occur, and indicate that sharing of the most frequent CDR3s among M-LAs of antigen-stimulated animals is an important feature of fish M-LAs. These findings support the notion of a high degree of reseeding and/or exchanges of common Ag-specific B cell clones among M-LAs induced during the same response. These properties of fish M-LAs show interesting commonalities with mammalian GCs operating in polyclonal settings. These GCs are seeded by several hundred naïve B cells, in particular when complex antigens are used (*30*). Furthermore, early secondary GCs after boost are re-seeded and diversified by a substantial number of naïve B cells in addition to memory B cells (*38, 39*). In such scenarios, the resulting GC reaction ends up with clonally diverse (polyclonal) GCs that include not only a few highly expanded high affinity B cell clones but also a large number of medium and low affinity B cell clones (*38*), and even B cell clones with no specificity for the Ag used for immunization (*40*). Moreover, and similar to what we show here for M-LAs, it has been reported that polyclonal GCs induced in the same response share also a significant number of their most frequent B cell clones (*30*), although only pairs of GCs were compared and the degree of clonotype sharing between those GCs was significantly lower than what we typically see when comparing the herein analyzed fish M-LAs. While M-LAs resemble those newly described polyclonal GCs, M-LAs would not contain medium or high

affinity B cell clones based on previous studies showing that affinity maturation of the Ab response in teleosts is poor (*17, 41*). Importantly, after infection we did not detect an M-LA in which the most frequent clones were not shared with other M-LAs. The later strongly suggests that polyclonal M-LAs are the norm in fish, whereas mammals contain those recently discovered
5 polyclonal GCs in addition to the well-known clonally homogenous GCs that contain only a few selected and highly expanded high affinity B cell clones due to intraclonal competition and as result of clonal burst processes (*25*).

We found that AID expression was mainly localized in M-LA B cells, a situation resembling that of mammalian AID which is known to be expressed at its highest levels in GC B cells (*25*).
10 It is known that within GCs, AID is responsible for 75% of apoptosis in DZ B cells, (*28*) and that apoptosis is considered an important mechanism required to counteract the large degree of B cell proliferation (*25*). Here we show that significant B cell apoptosis was only detected within M-LAs of infected animals thus suggesting that AID may also be a significant inducer of B cell apoptosis within M-LAs, and that apoptosis in these microstructures is an important mechanism
15 required to offset the high proliferation levels of M-LA B cells. Interestingly, we found that the percentatge B cells entering apoptosis in M-LAs was similar to that reported for GCs (2.6-5.7%).

While affinity maturation of Ig responses is generally poor in fish and other poikilotherms, evidence of SHM of Ag receptor genes have been reported in several species (*9, 42-46*). The high levels of AID expression detected in M-LA B cells of infected fish suggested that SHM
20 could be taking place within these cells. In support, our data show that M-LAs display significantly higher sequence variation in the CDR1-FR3 region of the V domain compared to non M-LAs areas, thus indicating the occurrence of SHM within these lymphoid microstructures. Most importantly, while CDR3 sharing analysis between M-LAs in the same spleen indicated

that large B cell clones after immunization likely move between these areas, our SHM studies showed also that shared lineages are the ones displaying the highest sequence variation. This prevalent concentration of SHM on shared lineages of M-LAs has not been described in any other vertebrate lymphoid microstructure, including GCs. A recent study found strong evidence of SHM taking place in MMCs from the head kidney (HK) in zebrafish (*47*). However, it remains to be determined whether SHM occurred in resident HK B cells responding to Ag, or if SHM occurred in plasmablast/plasma-like cells that migrated into the HK from inductive lymphoid tissue localized in the spleen or other lymphoid organs.

*please add a final overall conclusion sentence here. In conclusion, and in contrast to the current dogma stating the absence of GCs or analogous organized SLMS in cold-blooded vertebrates (3), here we show the existence of inducible teleost M-LAs with structural and functional features analogous to those of endothermic GCs. Further research is warranted to evaluate the evolutionary origins of M-LAs and GCs, and how these structures shape the ultimate diversity of antibody responses in polyclonal settings. Finally, it is also worparadigmth considering that since the overall structure of M-LAs is less organized than that of GCs, M-LAs might be more evolutionary related to immature TLOs, which contain loosely organized B and T cell zones and lack GCs (*48*). We propose that comparative studies of fish M-LAs (or equivalent cold-blooded SLM structures) may point to primordially conserved principles and/or convergent processes by which M-LAs, TLOs and the newly discovered polyclonal GCs are formed and regulated.

MATERIALS AND METHODS

Study design

The objective of this study was to determine how and where adaptive immune responses are induced in vertebrate species that lack germinal centers or analogous lymphoid structures. Immune responses were induced by parasite infection or through immunization with DNP-KLH. We used immunofluorescence (IF) microscopy to search the spleen for areas of antigen specific B cell and T cell proliferation which led to the identification of M-LAs. To determine the clonality of B cells we analyzed the IgM heavy chain (IgHμ) CDR3 repertoire of microdissected splenic M-LAs and non M-LA areas from infected and control fish. Through in situ hybridization studies we also determined whether M-LA B cells expressed activation-induced cytidine deaminase (AID), while through IF microscopy we analyzed the percentages of these cells undergoing apoptosis. To evaluate whether somatic hypermutation occur in M-LA B cells, we calculated the sequence variation of clonal set variants found within microdissected splenic M-LAs and non M-LA areas. Animal numbers per group are indicated in the respective figure legends. Sample sizes were chosen according to previous comparable studies conducted in our laboratory. Investigators were not blinded to groups. No data were excluded.

Fish husbandry

Rainbow trout (*Oncorhynchus mykiss*) were obtained from Troutlodge (Summer, WA) and were maintained as previously described by us (*18*). Fish (13 to 17 g) were acclimatized for 2 weeks at 15 °C in an aerated recirculating aquarium with internal biofilters and fed daily with dry

pellets at 1% biomass/day. All animal procedures were approved by the Institutional Animal Care and Use Committees of the University of Pennsylvania.

Ich parasite isolation and infection

Isolation of *Ichthyophthirius multifiliis* parasite (Ich) and Ich infections were performed as previously reported by us (*18, 19*). Briefly, for primary Ich infections, fish (n = 7) were exposed to Ich theronts (~1000 theronts per fish), and 8 to 10 days post exposure, infection was visually confirmed with the typical white spots (Ich trophonts) covering the skin and gills of the fish. Once the Ich trophonts detached from fish and no visible white spots were detected (~ 14 days after exposure), fish were transferred and quarantined in an Ich-free flow through tank for 2 weeks. Reinfection (secondary Ich exposure) of quarantined fish was conducted following the aforementioned protocol 4 weeks after the first exposure. Mock-infected fish (control fish) were kept in an Ich-free water tank following the same timelines used for Ich primary and secondary exposures. Both reinfected and control fish were euthanized 14 days after reinfection or mock-infection respectively with an overdose (300 mg/l) of tricaine methanesulfonate (MS-222; Syndel) as previously reported by us (*18, 19*). Spleen and sera from euthanized animals were collected as described below for further experiments. All analyses in this manuscript were performed on samples from reinfected fish and their respective mock-infected control animals.

Fish immunizations

Fish were immunized by intraperitoneal injection (i.p.) with 100 µg of Dinitropheny (DNP)-Keyhole limpet haemocyanin (KLH) (DNP-KLH; Millipore; 1 mg/ml in PBS, pH7.2) emulsified in Freund's complete adjuvant (Sigma-Aldrich). Four weeks after primary immunization, fish were boosted with the same amount of DNP-KLH emulsified in Freund's incomplete adjuvant (Sigma-Aldrich). Two weeks after the booster immunization, fish were euthanized as described

above. Control fish received 100 µl PBS mixed with the aforementioned adjuvants and were sampled following the same protocol. Sera and spleen tissue samples were collected as previously described by us (*18, 19*) or further experiments. All analyses below were performed on samples from boosted fish and their respective control animals.

5 *Specificity analysis of gp anti-trout CD4 pAb by flow cytometry*

Splenic leukocyte suspensions were obtained as previously described (*19, 49*). To evaluate the specificity of the newly produced gp anti-trout CD4 pAb, splenic leukocyte suspensions (1×10^6) were double stained with gp anti-trout CD4 pAb (1 µg/ml) and rat anti-trout CD4 mAb (clone 4.2.12, rat IgG2b; 5 µg/ml) (*49*). Primary antibodies were then detected with Alexa Fluor
10 647-conjugated goat anti-guinea pig IgG (Jackson ImmunoResearch) and PE-conjugated goat anti-rat IgG2b (Invitrogen) at 1 µg/ml each. To elucidate whether the gp anti-trout CD4 pAb showed any potential cross-reactivity IgM$^+$ B cells, splenic leukocytes (1×10^6) were stained with both anti-trout CD4 pAb (1 µg/ml) and biotinylated anti-trout IgM mAb (1 µg/ml). Primary antibodies were thereafter detected with Alexa Fluor 647-conjugated goat anti-guinea pig IgG
15 (Jackson ImmunoResearch) and Brilliant Violet 421 Streptavidin (Biolegend) at 1 µg/ml each. As isotype-matched controls for primary Abs, we used guinea pig IgG purified from pre-immune sera (1 µg/ml), and rat IgG2b (clone RTK4530, BioLegend; 5 µg/ml). Flow cytometry was performed using a FACSCanto cell analyzer (BD Biosciences), and data were analyzed using FlowJo software (FlowJo LLC).

20

Detection of antigen (Ag)- specific B cells by immunofluorescence microscopy and flow cytometry

The strategy on the methodology to detect Ag-specific B cells on spleen cryosections is shown in fig. S4. Ag-specific B cells were detected by immunofluorescence microscopy on spleen cryoblocks of DNP-KLH boosted fish and the respective control fish. Spleen cryoblocks were sectioned at a thickness of 10 μm and then fixed for 10 min in 2% PFA. The sections were thereafter permeabilized in 0.5% Tween 20 (Promega) in PBS (PBS-Tween, pH7.2) for 15 min at RT and then blocked with 2% bovine serum albumin (BSA, Gold Biotechnology) in PBS (PBS-BSA, pH7.2) for 30 min. In order to detect Ag-specific B cells, sections were then probed with DNP-phycoerythrin (DNP-PE; Millipore; 50μg/ml) for 2 hours at RT. After incubation with DNP-PE, sections were washed 3 times with PBS, and stained with anti-trout IgM mAb and anti-trout CD4 pAb followed by Alexa Fluor 488-conjugated goat anti-mouse IgG1 (Invitrogen) and Alexa Fluor 647-conjugated goat anti-guinea pig IgG (Invitrogen), respectively, as described above. Cell nuclei were stained with DAPI (1 μg/ml) before mounting with Fluoroshield. Images were acquired and analyzed using a Leica DM6000 fluorescence microscope or Leica SP8 confocal microscope and LAS X software. Percentage of M-LAs areas containing a high proportion of Ag-specific B cells from immunized and control fish where found by quantifying the percentage of M-LAs containing >10% of Ag-specific B cells in the spleen of infected and control fish.

To detect Ag-specific B cells by flow cytometry, spleen leukocytes from control and boosted fish were obtained as described above, and stained with DNP-PE (50 μg/ml) for 30 min at 4 °C in DMEM. Thereafter, cells were washed three times with DMEM and co-stained with mouse anti-trout IgM mAb (1 μg/ml) and gp anti-trout CD4 pAb (1 μg/ml) as described above. Positively stained IgM^+ and $CD4^+$ cells were detected with Alexa Fluor 488-conjugated goat anti-mouse IgG1 (Invitrogen) and Alexa Fluor 647-conjugated goat anti-guinea pig IgG

(Invitrogen), respectively at 2.5 μg/ml each. Flow cytometry was performed using a FACSCanto cell analyzer (BD Biosciences), and data were analyzed using FlowJo software (FlowJo LLC).

Laser capture microdissection (LCM) of M-LA and non M-LA areas and RNA extraction

5 The strategy on the methodology to identify and microdissect M-LA and non M-LA areas of spleen cryoblocks is depicted in fig S6. Cryoblocks of spleen from Ich reinfected fish, DNP-KLH boosted fish, and the respective control fish were serially sectioned (17 to 20 sections) at a thickness of 10μm and mounted onto PEN membrane slides (Leica). M-LA and non M-LA areas in these sections were identified as described in fig. S6, A and B. Sections containing the chosen 10 M-LA and non M-LA areas (corresponding to sections 2-6 from fig. S6B) were then fixed in ethanol (Sigma-Aldrich) and briefly washed in nuclease-free water (Sigma-Aldorich). The fixed sections were thereafter stained with HistoGene staining solution (Applied Biosystems) and dehydrated in a series of ethanol (70%, 90% and 100%). At this point sections were ready for microdissection with LCM system (LMD7000, Leica). Using the Leica software from LCM 15 apparatus, we quantified the exact area that was harvested for M-LAs, and these data was then used to harvest the same amount of area from a non M-LA regions of the same spleen section. The microdissected tissues were collected in a microtube containing Buffer RLT from the RNeasy Micro Kit (Qiagen), and total RNA from M-LA and non M-LA microdissected sections were extracted using the RNeasy Micro Kit according to the manufacturer's instructions. To 20 minimize RNA degradation, all procedures were performed quickly and under RNase free conditions

Production of guinea pig (gp) anti-trout CD4 polyclonal antibodies (pAbs)

To detect trout $CD4^+$ T cells on tissue cryosections by immunofluorescence microscopy and flow cytometry, we produced a pAb against trout CD4-2b. To this end, recombinant trout CD4-2b (CD4) was produced as a CD4/Fc fusion protein (Fc from mouse IgG2b) and purified as previously described by us (*20*). The recombinant protein was used to raise pAbs in guinea pigs by Cocalico Biologicals Inc. according to their standard protocols. Gp CD4-specific serum IgG titers from immunized animals were determined by ELISA as described in (*20*). Purification of IgG from gp serum was carried out as previously described by us (*20*) with some protocol modifications. Briefly, total gp IgG was purified from antisera or pre-immune sera using a HiTrap protein A column (GE Healthcare) according to the manufacturer's instructions. The purified total IgG from antisera was then passed through an in-house mouse IgG2b-affinity column to remove pAbs recognizing Fc from mouse IgG2b. The resulting flow through fraction was then applied to an in-house CD4/Fc fusion protein-affinity column to purify CD4-specific gp IgG. Specificity of affinity purified gp anti-trout CD4 IgG against trout CD4 was determined by ELISA, flow cytometry and immunofluorescence microscopy following the same methodologies described by us in (*20,49*) .

Statistical analysis

The sample size and number of independent experiments are indicated in the figure captions. Histological evaluations and cell counting were performed by two independent researchers. No data were excluded. Unpaired Student's *t* test, one-way and two-way ANOVAs followed by Tukey's multiple comparison test were performed in Prism (GraphPad) for analysis of differences between groups. *P* values of 0.05 or less were considered statistically significant.

Supplementary Materials:

Materials and Methods

Fig.S1-S6

Tables S1-S2

5 Raw data excel file: Supplementary data file S1

References and Notes:

1. D. Parra, F. Takizawa, J. O. Sunyer, Evolution of B cell immunity. *Annu. Rev. Anim. Biosci.* **1**, 65-97 (2013).
2. M. Hirano, S. Das, P. Guo, M. D. Cooper, The evolution of adaptive immunity in vertebrates. *Adv. Immunol.* **109**, 125-157 (2011).
3. M. F. Flajnik, A cold-blooded view of adaptive immunity. *Nat. Rev. Immunol.* **18**, 438-453 (2018).
4. J. Hofmann, M. Greter, L. Du Pasquier, B. Becher, B-cells need a proper house, whereas T-cells are happy in a cave: the dependence of lymphocytes on secondary lymphoid tissues during evolution. *Trends Immunol.* **31**, 144-153 (2010).
5. A. A. Zarrin, F. W. Alt, J. Chaudhuri, N. Stokes, D. Kaushal, L. Du Pasquier, M. Tian, An evolutionarily conserved target motif for immunoglobulin class-switch recombination. *Nat. Immunol.* **5**, 1275-1281 (2004).
6. M. Yasuda, Y. Taura, Y. Yokomizo, S. Ekino, A comparative study of germinal center: fowls and mammals. *Comp. Immunol. Microbiol. Infect. Dis.* **21**, 179-189 (1998).
7. V. M. Barreto, B. G. Magor, Activation-induced cytidine deaminase structure and functions: a species comparative view. *Dev. Comp. Immunol.* **35**, 991-1007 (2011).
8. S. Marr, H. Morales, A. Bottaro, M. Cooper, M. Flajnik, J. Robert, Localization and differential expression of activation-induced cytidine deaminase in the amphibian *Xenopus* upon antigen stimulation and during early development. *J. Immunol.* **179**, 6783-6789 (2007).

9. F. Yang, G. C. Waldbieser, C. J. Lobb, The nucleotide targets of somatic mutation and the role of selection in immunoglobulin heavy chains of a teleost fish. *J. Immunol.* **176**, 1655-1667 (2006).

10. A. E. Marianes, A. M. Zimmerman, Targets of somatic hypermutation within immunoglobulin light chain genes in zebrafish. *Immunology* **132**, 240-255 (2011).

11. C. M. Press, B. H. Dannevig, T. Landsverk, Immune and enzyme histochemical phenotypes of lymphoid and nonlymphoid cells within the spleen and head kidney of Atlantic salmon (*Salmo salar* L.). *Fish Shellfish Immunol.* **4**, 79-93 (1994).

12. R. Bermudez, F. Vigliano, A. Marcaccini, A. Sitja-Bobadilla, M. I. Quiroga, J. M. Nieto, Response of Ig-positive cells to *Enteromyxum scophthalmi* (Myxozoa) experimental infection in turbot, *Scophthalmus maximus* (L.): A histopathological and immunohistochemical study. *Fish Shellfish Immunol.* **21**, 501-512 (2006).

13. N. C. Steinel, D. I. Bolnick, Melanomacrophage centers as a histological indicator of immune function in fish and other poikilotherms. *Front Immunol.* **8**, 827 (2017).

14. Z. S. Gyimesi, E. W. Howerth, Severe melanomacrophage hyperplasia in a crocodile lizard, *Shinisaurus crocodilurus*: a review of melanomacrophages in ectotherms. *J. Herpetol. Med. Surg.* **14**, 19-23 (2004).

15. C. Agius, R. J. Roberts, Melano-macrophage centres and their role in fish pathology. *J. Fish. Dis.* **26**, 499-509 (2003).

16. H. W. Ferguson, The relationship between ellipsoids and melano-macrophage centres in the spleen of turbot (*Scophthalmus maximus*). *J. Comp. Pathol.* **86**, 377-380 (1976).

17. J. O. Sunyer, P. Boudinot, "B-Cell Responses and Antibody Repertoires in Teleost Fish: From Ag Receptor Diversity to Immune Memory and Vaccine Development" in *Principles*

of Fish Immunology : From Cells and Molecules to Host Protection, K. Buchmann, C. J. Secombes, Eds. (Springer, Cham, 2022), pp. 253-278.

18. Z. Xu, F. Takizawa, E. Casadei, Y. Shibasaki, Y. Ding, T. J. C. Sauters, Y. Yu, I. Salinas, J. O. Sunyer, Specialization of mucosal immunoglobulins in pathogen control and microbiota homeostasis occurred early in vertebrate evolution. *Sci. Immunol.* **5**, eaay3254 (2020).
19. Z. Xu, F. Takizawa, D. Parra, D. Gomez, L. von Gersdorff Jorgensen, S. E. LaPatra, J. O. Sunyer, Mucosal immunoglobulins at respiratory surfaces mark an ancient association that predates the emergence of tetrapods. *Nat. Commun.* **7**, 10728 (2016).
20. Y. A. Zhang, I. Salinas, J. Li, D. Parra, S. Bjork, Z. Xu, S. E. LaPatra, J. Bartholomew, J. O. Sunyer, IgT, a primitive immunoglobulin class specialized in mucosal immunity. *Nat. Immunol.* **11**, 827-835 (2010).
21. C. F. Sales, R. F. Silva, M. G. Amaral, F. F. Domingos, R. I. Ribeiro, R. G. Thomé, H. B. Santos, Comparative histology in the liver and spleen of three species of freshwater teleost. *Neotrop. Ichthyol.* **15**, (2017).
22. B. S. Steiniger, Human spleen microanatomy: why mice do not suffice. *Immunology* **145**, 334-346 (2015).
23. R. Fänge, S. Nilsson, The fish spleen: structure and function. *Experientia* **41**, 152-158 (1985).
24. P. Garside, E. Ingulli, R. R. Merica, J. G. Johnson, R. J. Noelle, M. K. Jenkins, Visualization of specific B and T lymphocyte interactions in the lymph node. *Science* **281**, 96-99 (1998).

25. G. D. Victora, M. C. Nussenzweig, Germinal Centers. *Annu. Rev. Immunol.* **40**, 413-442 (2022).

26. Y. Mizutani, S. Tsuge, K. Shiogama, R. Shimomura, S. Kamoshida, K. Inada, Y. Tsutsumi, Enzyme-labeled antigen method: histochemical detection of antigen-specific antibody-producing cells in tissue sections of rats immunized with horseradish peroxidase, ovalbumin, or keyhole limpet hemocyanin. *J. Histochem. Cytochem.* **57**, 101-111 (2009).

27. M. Cossarini-Dunier, F. X. Desvaux, M. Dorson, Variability in humoral responses to DNP-KLH of rainbow trout (*Salmo gairdneri*). Comparison of antibody kinetics and immunoglobulins spectrotypes between normal trouts and trouts obtained by gynogenesis or self-fertilization. *Dev. Comp. Immunol.* **10**, 207-217 (1986).

28. C. T. Mayer, A. Gazumyan, E. E. Kara, A. D. Gitlin, J. Golijanin, C. Viant, J. Pai, T. Y. Oliveira, Q. Wang, A. Escolano, M. Medina-Ramirez, R. W. Sanders, M. C. Nussenzweig, The microanatomic segregation of selection by apoptosis in the germinal center. *Science* **358**, eaao2602 (2017).

29. A. Sepahi, A. Kraus, E. Casadei, C. A. Johnston, J. Galindo-Villegas, C. Kelly, D. Garcia-Moreno, P. Munoz, V. Mulero, M. Huertas, I. Salinas, Olfactory sensory neurons mediate ultrarapid antiviral immune responses in a TrkA-dependent manner. *Proc. Natl. Acad. Sci. U. S. A.* **116**, 12428-12436 (2019).

30. J. M. Tas, L. Mesin, G. Pasqual, S. Targ, J. T. Jacobsen, Y. M. Mano, C. S. Chen, J. C. Weill, C. A. Reynaud, E. P. Browne, M. Meyer-Hermann, G. D. Victora, Visualizing antibody affinity maturation in germinal centers. *Science* **351**, 1048-1054 (2016).

31. T. Arulraj, S. C. Binder, P. A. Robert, M. Meyer-Hermann, Germinal Centre Shutdown. *Front. Immunol.* **12**, 705240 (2021).

32. M. Y. Zeng, D. Cisalpino, S. Varadarajan, J. Hellman, H. S. Warren, M. Cascalho, N. Inohara, G. Nunez, Gut Microbiota-Induced Immunoglobulin G Controls Systemic
5 Infection by Symbiotic Bacteria and Pathogens. *Immunity* **44**, 647-658 (2016).

33. I. Salinas, A. Fernandez-Montero, Y. Ding, J. O. Sunyer, Mucosal immunoglobulins of teleost fish: A decade of advances. *Dev. Comp. Immunol.* **121**, 104079 (2021).

34. Z. Xu, D. Parra, D. Gómez, I. Salinas, Y.A, Zhang, L. von Gersdorff Jørgensen, R. D. Heinecke, K. Buchmann, S. LaPatra, J. O. Sunyer, Teleost skin, an ancient mucosal surface
10 that elicits gut-like immune responses. *Proc. Natl. Acad. Sci. U. S. A.* **110**, 13097-13102 (2013).

35. B. Garcia, F. Dong, E. Casadei, J. Rességuier, J. Ma, K. D. Cain, P. A. Castrillo, Z. Xu, I. Salinas, A Novel Organized Nasopharynx-Associated Lymphoid Tissue in Teleosts That Expresses Molecular Markers Characteristic of Mammalian Germinal Centers. *J. Immunol.*
15 **209**, 2215-2226 (2022).

36. H. Matz, R. S. Taylor, A. K. Redmond, T. M. Hill, R. R. Daniels, M. Beltran, N. C. Henderson, D. J. Macqueen, and H. Dooley. Organized B cell sites in cartilaginous fishes reveal the evolutionary foundation of germinal centers. *Cell Reports* **42**, 112664 (2023).

37. H. R. Neely, J. Guo, E. M. Flowers, M. F. Criscitiello, M. F. Flajnik, "Double-duty"
20 conventional dendritic cells in the amphibian *Xenopus* as the prototype for antigen presentation to B cells. *Eur. J. Immunol.* **48**, 430-440 (2018).

38. L. Mesin, A. Schiepers, J. Ersching, A. Barbulescu, C. B. Cavazzoni, A. Angelini, T. Okada, T. Kurosaki, G. D. Victora, Restricted Clonality and Limited Germinal Center

Reentry Characterize Memory B Cell Reactivation by Boosting. *Cell* **180**, 92-106 e11 (2020).

39. J. S. Turner, J. Q. Zhou, J. Han, A. J. Schmitz, A. A. Rizk, W. B. Alsoussi, T. Lei, M. Amor, K. M. McIntire, P. Meade, S. Strohmeier, R. I. Brent, S. T. Richey, A. Haile, Y. R. Yang, M. K. Klebert, T. Suessen, S. Teefey, R. M. Presti, F. Krammer, S. H. Kleinstein, A. B. Ward, A. H. Ellebedy, Human germinal centres engage memory and naive B cells after influenza vaccination. *Nature* **586**, 127-132 (2020).

40. C. Gregoire, L. Spinelli, S. Villazala-Merino, L. Gil, M. P. Holgado, M. Moussa, C. Dong, A. Zarubica, M. Fallet, J. M. Navarro, B. Malissen, P. Milpied, M. Gaya, Viral infection engenders bona fide and bystander subsets of lung-resident memory B cells through a permissive mechanism. *Immunity* **55**, 1216-1233 e1219 (2022).

41. J. Ye, I. M. Kaattari, S. L. Kaattari, The differential dynamics of antibody subpopulation expression during affinity maturation in a teleost. *Fish Shellfish Immunol.* **30**, 372-377 (2011).

42. M. Wilson, E. Hsu, A. Marcuz, M. Courtet, L. Du Pasquier, C. Steinberg, What limits affinity maturation of antibodies in Xenopus -- the rate of somatic mutation or the ability to select mutants? *EMBO J.* **11**, 4337-4347 (1992).

43. K. R. Hinds-Frey, H. Nishikata, R. T. Litman, G.W. Litman, Somatic variation precedes extensive diversification of germline sequences and combinatorial joining in the evolution of immunoglobulin heavy chain diversity. *J. Exp. Med.* **178**, 815-824 (1993).

44. M. Diaz, A. S. Greenberg, M. F. Flajnik, Somatic hypermutation of the new antigen receptor gene (NAR) in the nurse shark does not generate the repertoire: possible role in

antigen-driven reactions in the absence of germinal centers. *Proc. Natl. Acad. Sci. U. S. A.* **95**, 14343-14348 (1998).

45. S. S. Lee, D. Tranchina, Y. Ohta, M. F. Flajnik, E. Hsu, Hypermutation in shark immunoglobulin light chain genes results in contiguous substitutions. *Immunity* **16**, 571-582 (2002).

46. N. Jiang, J. A. Weinstein, L. Penland, R. A. 3rd White, D. S.Fisher, S. R. Quake, Determinism and stochasticity during maturation of the zebrafish antibody repertoire. *Proc. Natl. Acad. Sci. U. S. A.* **108**, 5348-5353 (2011).

47. D. Waly, A. Muthupandian, C.-W. Fan, H. Anzinger, B. G. Magor, Immunoglobulin VDJ repertoires reveal hallmarks of germinal centers in unique cell clusters isolated from zebrafish (*Danio rerio*) lymphoid tissues. *Front. Immunol.* **13**, 7032 (2022).

48. K. Neyt, F. Perros, C. H. GeurtsvanKessel, H. Hammad, B. N. Lambrecht, Tertiary lymphoid organs in infection and autoimmunity. *Trends Immunol.* **33**, 297-305 (2012).

49. F. Takizawa, S. Magadan, D. Parra, Z. Xu, T. Korytar, P. Boudinot, J. O. Sunyer, Novel Teleost CD4-Bearing Cell Populations Provide Insights into the Evolutionary Origins and Primordial Roles of $CD4^+$ Lymphocytes and $CD4^+$ Macrophages. *J. Immunol.* **196**, 4522-4535 (2016).

50. S. Magadan, A. Krasnov, S. Hadi-Saljoqi, S. Afanasyev, S. Mondot, D. Lallias, R. Castro, I. Salinas, J. O. Sunyer, J. Hansen, B.F. Koop, M.P. Lefranc, P. Boudinot, Standardized IMGT® nomenclature of salmonidae IGH genes, the paradigm of Atlantic salmon and rainbow trout: from genomics to repertoires. *Front. Immunol.* **10**, 2541 (2019).

51. S. Magadan, S. Mondot, Y. Palti, G. Gao, M. P. Lefranc, P. Boudinot, Genomic analysis of a second rainbow trout line (Arlee) leads to an extended description of the IGH VDJ gene repertoire. *Dev. Comp. Immunol.* **118**, 103998 (2021).

52. J. A. Ott JA, C.D. Castro, T.C. Deiss, Y. Ohta, M.F. Flajnik, M.F. Criscitiello, Somatic
5 hypermutation of T cell receptor α chain contributes to selection in nurse shark thymus. *Elife* **7**, e28477 (2018).

53. D. DeLuca, M. Wilson, G. W. Warr, Lymphocyte heterogeneity in the trout, *Salmo gairdneri*, defined with monoclonal antibodies to IgM. *Eur. J. Immunol.* **13**, 546-551 (1983).

10 54. V. Lambert, J. Lecomte, S. Hansen, S. Blacher, M. L. Gonzalez, I. Struman, N. E. Sounni, E. Rozet, P. de Tullio, J. M. Foidart, J. M. Rakic, A. Noel, Laser-induced choroidal neovascularization model to study age-related macular degeneration in mice. *Nat. Protoc.* **8**, 2197-2211 (2013).

55. F. Ke, Z. L. Benet, M. P. Maz, J. Liu, A. L. Dent, J. M. Kahlenberg, I. L. Grigorova,
15 Germinal center B cells that acquire nuclear proteins are specifically suppressed by follicular regulatory T cells. *Elife* **12**, e83908 (2023).

56. E. Shen, H. Rabe, L. Luo, L. Wang, Q. Wang, J. Yin, X. Yang, W. Liu, J. M. Sido, H. Nakagawa, L. Ao, H. J. Kim, H. Cantor, J. W. Leavenworth, Control of germinal center localization and lineage stability of follicular regulatory T cells by the Blimp1 transcription
20 factor. *Cell Rep.* **29**, 1848-1861. e1846 (2019).

57. J. Schindelin, I. Arganda-Carreras, E. Frise, V. Kaynig, M. Longair, T. Pietzsch, S. Preibisch, C. Rueden, S. Saalfeld, B. Schmid, J. Y. Tinevez, D. J. White, V. Hartenstein,

K. Eliceiri, P. Tomancak, A. Cardona, Fiji: an open-source platform for biological-image analysis. *Nat. Methods* **9**, 676-682 (2012).

Acknowledgments: J.O.S. dedicates this manuscript to the loving memory of his father, who recently passed away. His incessant encouragement, love and quest for continuous improvement has deeply influenced my life, including this work. We thank S. Prouty and the Penn Skin Biology and Diseases Resource-based Center, funded by NIH/NIAMS grant P30-AR069589 and the University of Pennsylvania Perelman School of Medicine for the help provided with the Laser Capture Microdissection; G. Ruthel of PennVet Imaging Core and Nihon University general research institute for help with microscope analysis; the personnel of the University Laboratory Animal Resources (ULAR) of the University of Pennsylvania for their invaluable help in the daily husbandry of our Rainbow Trout; Dr. A. Carty for the excellent veterinary care of the fish; Dr. D. Stefanovski (School of Veterinary Medicine, University of Pennsylvania) and Dr. A. Serradell (University of Las Palmas, Spain) for their advice in statistical analysis of this study.

Funding:

National Institutes of Health 2R01GM085207-09 (JOS)

U.S. Department of Agriculture grant USDA-NIFA 2020-06446 (JOS)

U.S. Department of Agriculture grant USDA-NIFA 2021-06961 (JOS)

Japan Society for the Promotion of Science Overseas Research Fellowship (YS)

Japan Society for the Promotion of Science KAKENHI 20K22594 (YS)

Japan Society for the Promotion of Science KAKENHI 21H02288 (YS, FT)

Japan Society for the Promotion of Science KAKENHI 20KK0144 (YS, FT)

National Natural Science Foundation of China 31802337 (YD)

Author contributions: JOS, PB, AK designed the study. YS, AFM, SW, JML, FF performed the immunization of fish and sample collection. YS, AFM conducted ISH/IF staining and immunofluorescence microscope. YS and SW performed LCM and RNA extraction. SA, AK and PB performed CDR3 Illumina sequencing, and bioinformatic analyses. YS and YD performed flow cytometry. FT and YD performed antibody production and purification. JOS wrote the manuscript with feedback from all authors. JOS, PB, YD, YS, JL and AFM edited the manuscript. JOS supervised the project.

Competing interests: Authors declare that they have no competing interests.

Data and materials availability: All data are available in the main text or the supplementary materials. Sequence data used in this work are deposited at the BioProject National Center for Biotechnology Information database with the SRA accession number PRJNA854339 (https://www.ncbi.nlm.nih.gov/bioproject/854339). The newly generated guinea pig anti-trout CD4 polyclonal antibodies can be provided by J.O.S. pending a completed material transfer agreement. All data needed to evaluate the conclusions in the paper are present in the paper and/or the Supplementary Materials.

Figures and Legends

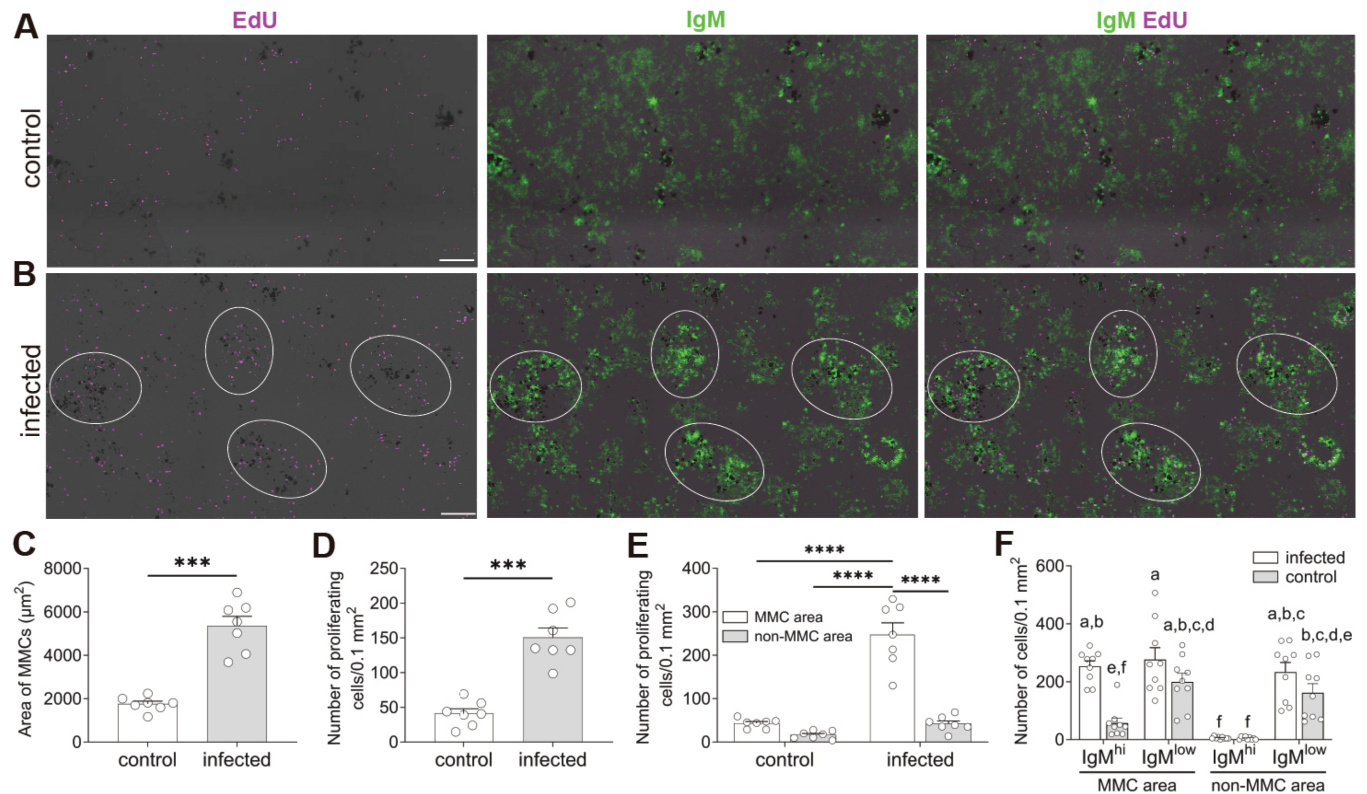

Fig. 1. Intense IgM⁺ B cell proliferation occurs nearby splenic melanomacrophage centers (MMCs) upon infection. (**A** and **B)** Immunofluorescence analysis of EdU incorporation

5 by cells of spleen from control (A) or infected fish (B). Spleen cryosections were stained for EdU (magenta) and IgM (green). Groups of dark cells in all images represent MMCs. White circles in (B) outline MMC-adjacent areas with high cell proliferation. Scale bars, 100 μm. (**C** and **D**) Area of MMCs, defined as the total surface of melanomacrophages (C), and number of proliferating cells (D) calculated from spleen cryosections of control

10 or infected fish (n = 7). (**E**) Number of proliferating cells in MMC- and non-MMC areas of spleen cryosections from control or infected fish (n = 7). (**F**) Number of IgM^{hi} and IgM^{low} B cells in MMC- and non-MMC areas of spleen cryosections from control or

infected fish (n = 9). Data in (C to F) are representative of at least three independent experiments (mean and SEM). Empty circles represent values from individual fish. Statistical analyses were performed by unpaired Student's t test (C and D) or two-way ANOVA followed by Tukey's post hoc test (E and F). ***$P < 0.001$, ****$P < 0.0001$.

5 Plot bars of (F) not sharing common letters are significantly different ($P < 0.05$).

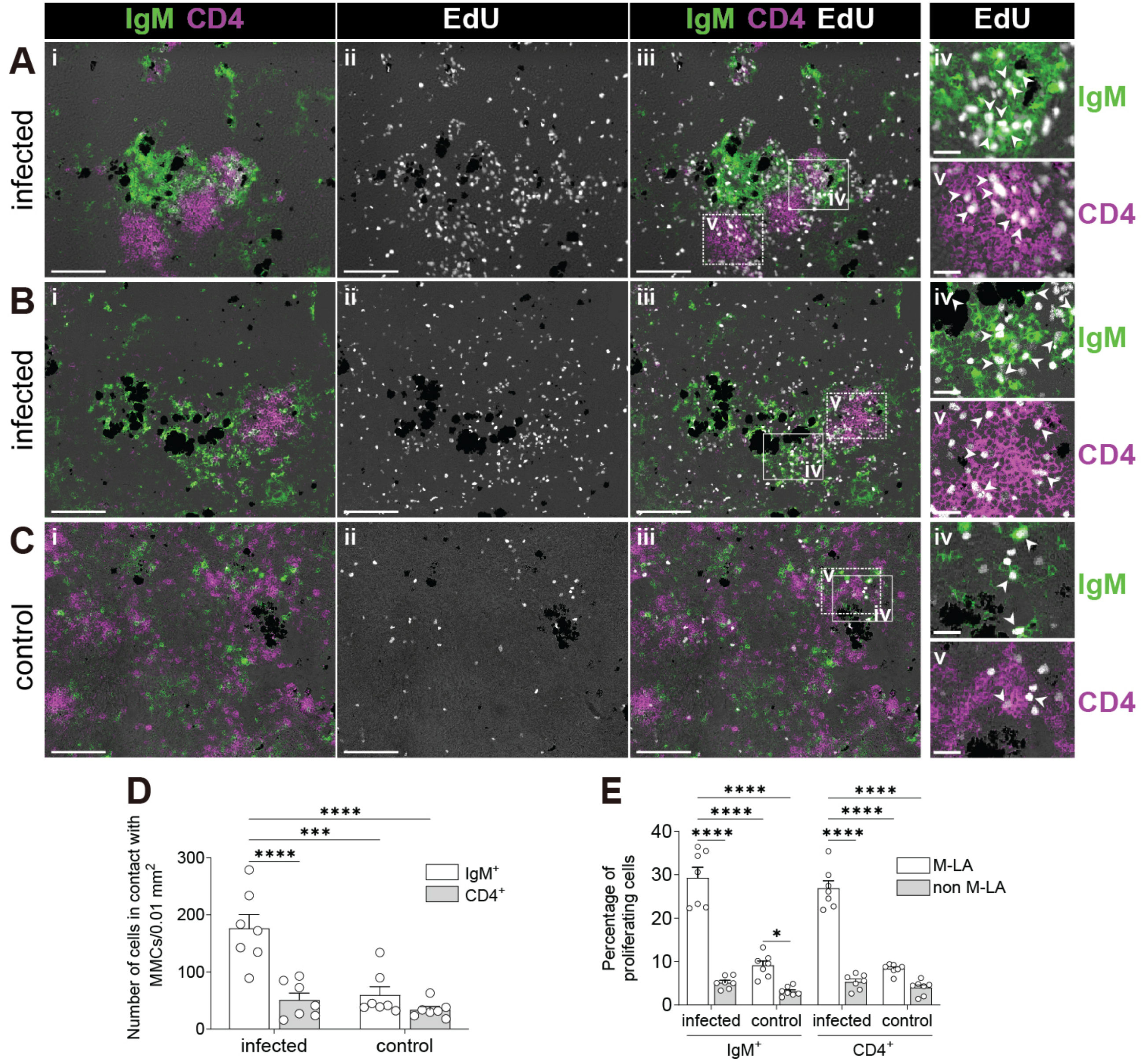

Fig. 2. Aggregates of highly proliferating splenic IgM⁺ B cells and CD4⁺ T cells are induced nearby MMCs upon infection. (**A** to **C**) Immunofluorescence analysis of EdU incorporation by IgM⁺ B cells and CD4⁺ T cells from MMC-associated lymphoid aggregates (M-LAs) of spleen from infected (A and B) and control fish (C). Spleen cryosections were stained for IgM (green), CD4 (magenta) and EdU (white). (**A** to **C**) Image in (i) shows a representative M-LA stained for IgM (green) and CD4 (magenta); (ii

and iii) show the same tissue area of (i) stained for EdU (white) (ii), IgM (green), CD4 (magenta) and EdU (white) (iii); (iv and v) show enlarged images of the areas outlined in (iii) displaying proliferating (EdU$^+$) IgM$^+$ B cells (iv) and proliferating (EdU$^+$) CD4$^+$ T cells (v). White arrowheads point to examples of proliferating IgM$^+$ B cells and CD4$^+$ T cells. Scale bars, 100 μm (i to iii), 20 μm (iv and v). Groups of dark cells in all images represent MMCs. Data is representative of at least three independent experiments. (**D**) Number of IgM$^+$ B cells and CD4$^+$ T cells in contact with MMCs of spleen cryosections from control or infected fish. (**E**) Percentage of proliferating IgM$^+$ B cells and CD4$^+$ T cells in M-LA and non M-LA areas of spleen cryosections from control or infected fish. Data is representative of at least three independent experiments (mean and SEM). Empty circles represent values from individual fish ($n = 7$). Statistical analyses were performed by two-way ANOVA followed by Tukey's post hoc test. *$P < 0.05$, ***$P < 0.001$, ****$P < 0.0001$.

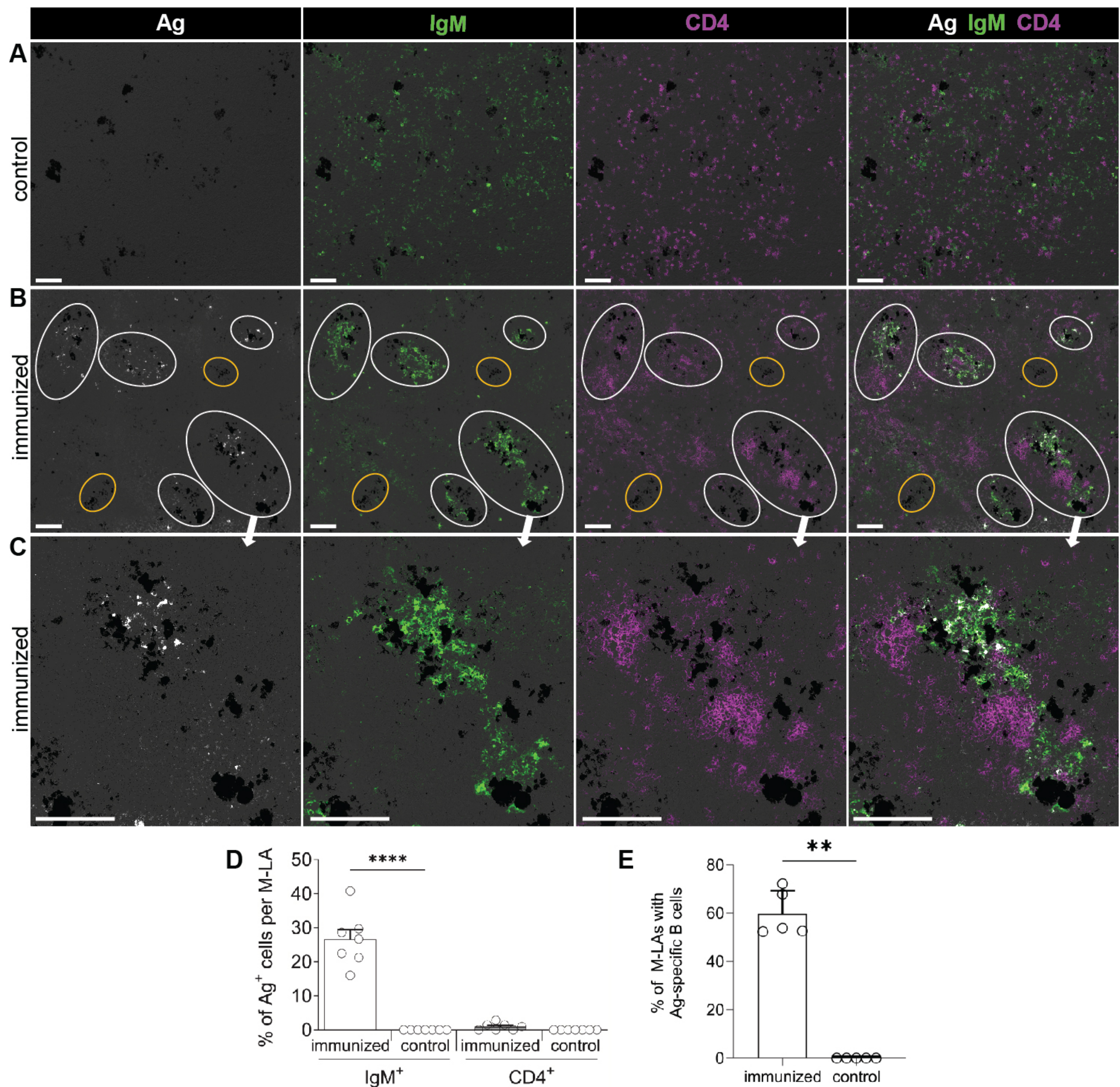

Fig. 3. Ag-specific B cells are mostly localized within M-LAs of immunized fish. (**A** to **C**) Immunofluorescence analysis of Ag-specific cells in spleen of control fish (A) and immunized fish (B and C). Spleen cryosections were probed with DNP-PE (white)

5 followed by detection of IgM (green) and CD4 (magenta). White circles outline M-LAs

containing Ag-specific B cells while yellow circles outline MMCs lacking B- and T cell zones and Ag-specific cells. Scale bars, 100 µm. Groups of dark cells in all images represent MMCs. (**D**) Percentage of IgM$^+$ B cells and CD4$^+$ T cells positive for DNP-PE in M-LAs and non M-LA areas from immunized and control fish. Empty circles represent values from individual fish ($n = 7$). (**E**) Percentage of M-LAs areas containing a high proportion (>10%) of Ag-specific B cells from immunized and control fish. Empty circles represent values from individual fish ($n = 5$). Data is representative of at least three independent experiments (mean and SEM). Statistical analyses were performed by one-way ANOVA followed by Tukey's post hoc test (D) (D) and Mann-Whitney test (E). $^{**}P < 0.01$, $^{****}P < 0.0001$.

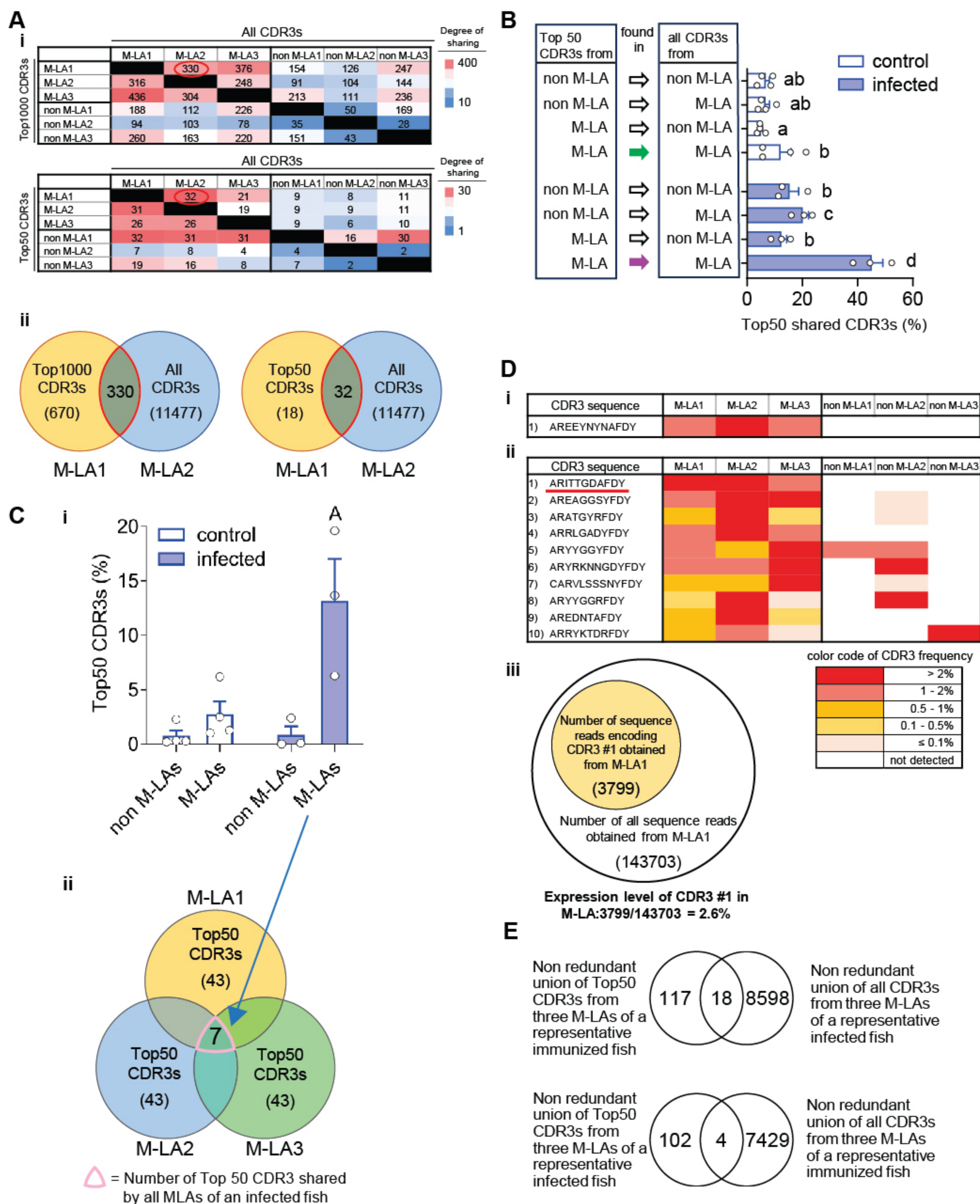

Fig. 4. IgHμ repertoire analysis shows that M-LAs from infected fish share a significant proportion of their most frequent CDR3s. M-LAs and non M-LA areas from the

spleen of infected and control fish were microdissected and their IgM heavy chain (IgHμ) clonal composition was determined by CDR3 repertoire analysis. (**A**) Pairwise comparison of the most frequent CDR3s from three M-LAs and three non M-LA areas of a representative infected fish. (i) matrix displaying the numbers of the most frequent CDR3s (Top1000 [upper panel] or Top50 [lower panel]) from M-LA or non M-LA areas (rows) present in (i.e., shared by) each M-LA or non M-LA area (columns). Heatmap shows graded colors from intense red (high CDR3 sharing) to intense blue (low CDR3 sharing). Graphical illustrations (ii) of representative matrix values (red-circled numbers in [i]). Left illustration shows that 330 CDR3s are shared between the Top1000 CDR3s from M-LA1 and all identified CDR3s (11477) from M-LA2, while the right illustration shows that 18 CDR3s are shared between the Top50 CDR3s from M-LA1 and all identified CDR3s (11477) from M-LA2. (**B**) Bar plots represent statistics of the same analysis as in (A) for several fish, and show the mean percentage of the Top50 CDR3s from M-LAs or non M-LA areas found in (i.e., shared by) M-LAs or non M-LA areas from the same spleen. Plot bars show mean values, error bars show SEM. Control fish (white bars), $n = 4$; infected fish (blue bars), $n = 3$. Empty circles represent values from individual fish. Statistical analyses were performed by two-way ANOVA followed by Tukey's post hoc test. Plot bars not sharing common letters are significantly different ($P<0.05$). Green and magenta arrows point to the Top50 CDR3s from M-LAs found in all CDR3s from M-LAs of control and infected fish respectively. (**C**) Proportion of the Top50 CDR3s shared by all M-LAs or all non M-LA areas within the same spleen. Values in bar plot (i) represent the mean % of the Top 50 CDR3s shared by all M-LAs or non M-LA areas of the same spleen from infected ($n = 3$) and control fish ($n = 4$), error

bars show SEM. Empty circles represent values from individual fish. Values were generated from the same datasets as for panel (B). Statistical analyses were performed by two-way ANOVA followed by Tukey's post hoc test; Plot bar with the letter A above is significantly different with the other groups ($P < 0.05$). (ii) depicts a graphical illustration
5 representing the number of Top50 CDR3s (7) shared by 3 M-LAs of a representative fish, thus indicating that those three M-LAs share 14% of their Top50 CDR3s. (**D**) Color-coded representation of the frequency (i.e., expression level) of the Top50 CDR3s (left column) found in all M-LAs from one representative control (i) or infected (ii) fish. Graphical illustration (iii) representing the number of illumina sequence reads (3799) for
10 CDR3 #1 (underlined in D[ii]) detected in M-LA1 (i.e, that number of sequence reads represent 2.6% of all the CDR3 reads (143703) sequenced from M-LA1 of a representative infected fish). (**E**) Upper panel depicts a Venn diagram showing the intersect between the Top50 CDR3s detected in three M-LAs of a representative immunized DNP-KLH fish and all CDR3s detected in three M-LAs from an infected fish,
15 while the lower panel depicts a Venn diagram showing the intersect between the Top50 CDR3s detected in three M-LAs from a representative infected fish and all CDR3s detected in three M-LAs from a fish immunized with DNP-KLH.

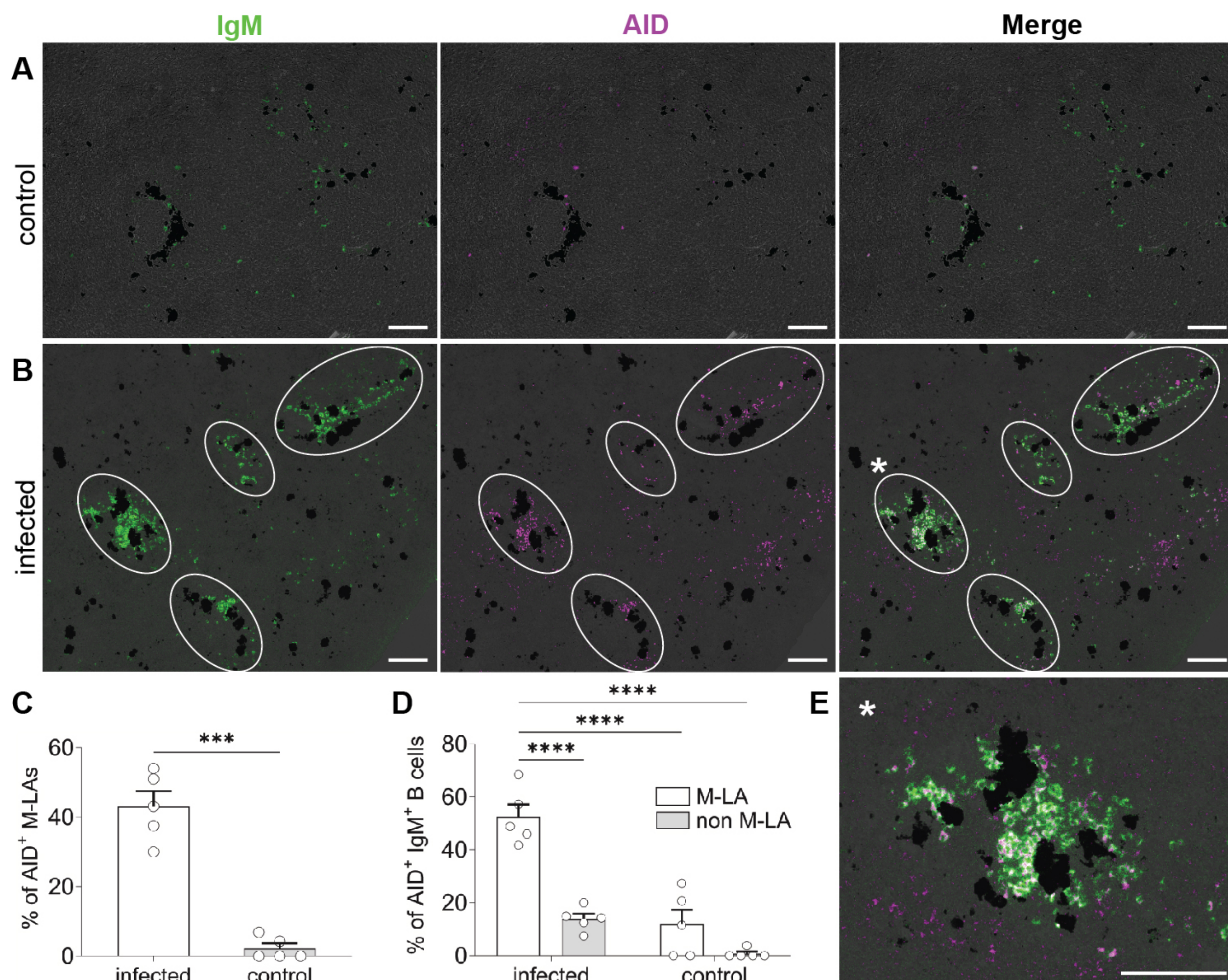

Fig. 5. IgM⁺ B cells from M-LAs of infected fish express high levels of AID. (**A** and **B**)

Representative double *in situ* hybridization images of trout AID and IgM from spleen of control (A) or infected fish (B). Spleen cryosections were hybridized with IgM (green)

5 and AID (magenta) antisense probes. White circles represent M-LAs containing IgM^+ and AID^+ cells. AID^+IgM^+ cells are seen as white cells in Merged images. (**C**) Percentage of M-LAs from infected and control fish containing significant numbers of AID^+ cells. M-LAs were considered AID^+ when containing more than 10 AID^+ cells per M-LA. (**D**) Percentage of AID^+IgM^+ B cells from M-LA and non M-LA areas of infected and control

10 fish. (**E**) Enlarged M-LA from (B) (enlarged M-LA from Merged image of (B) is marked

with a white asterisk). Scale bars, 100 µm. Groups of dark cells in all images represent MMCs. Data are representative of at least three independent experiments (mean and SEM). Empty circles represent values from individual fish ($n = 5$). Statistical analyses were performed by unpaired Student's t test (C) or two-way ANOVA followed by

5 Tukey's post hoc test (D). $^{***}P < 0.001$, $^{****}P < 0.0001$.

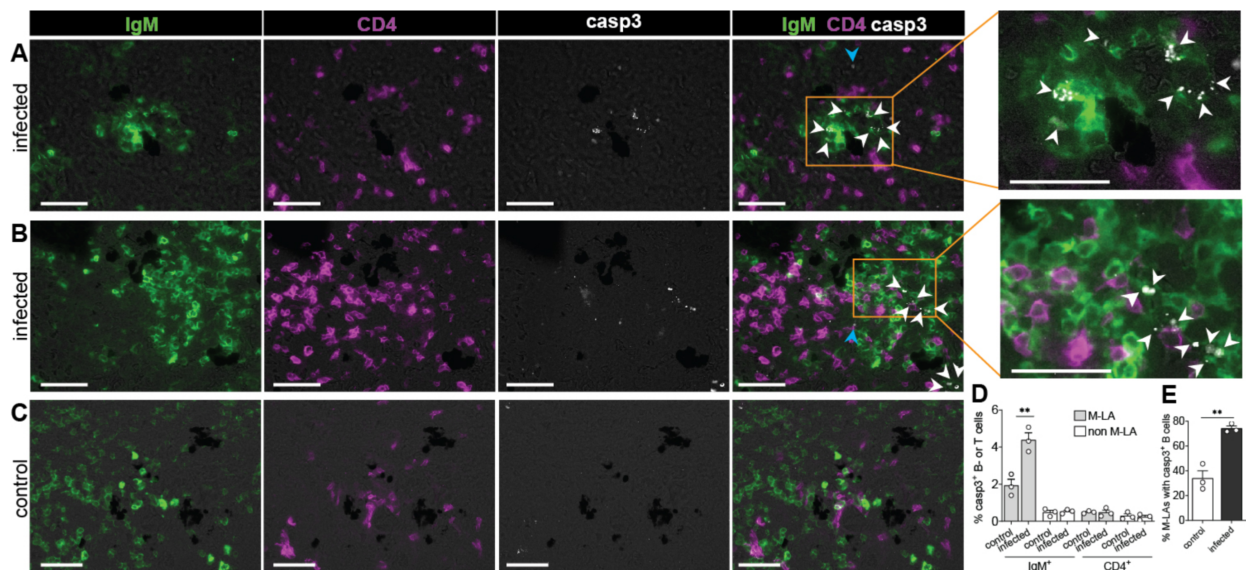

Fig. 6. M-LA B cells undergo significant apoptosis upon infection. Immunofluorescence analysis of activated caspase 3 (casp3) staining in M-LA and non M-LA areas of spleen from infected and control fish. (**A** to **C**) Representative M-LAs from infected (A and B) and control (C) fish stained for IgM (green), CD4 (magenta) and casp3 (white). The right panels of A and B represent enlarged images from areas outlined in orange. Scale bars, 50 µm. White triangles point to casp3$^+$IgM$^+$ cells, while blue triangles point to casp3$^+$CD4$^-$IgM$^-$ cells. (**D**) Percentage of casp3$^+$IgM$^+$ and casp3$^+$CD4$^+$ cells in M-LA and non M-LA areas from control and infected fish. (**E**) Percentage of M-LAs with casp3$^+$ B cells in control and infected fish. Data are representative of at least three independent experiments. The bars of the graphs represent the mean (n = 3) and the error bars the SEM (D and E), empty circles represent values from individual fish. Statistical analyses were performed by unpaired Student's t test. $^{**}P < 0.01$.

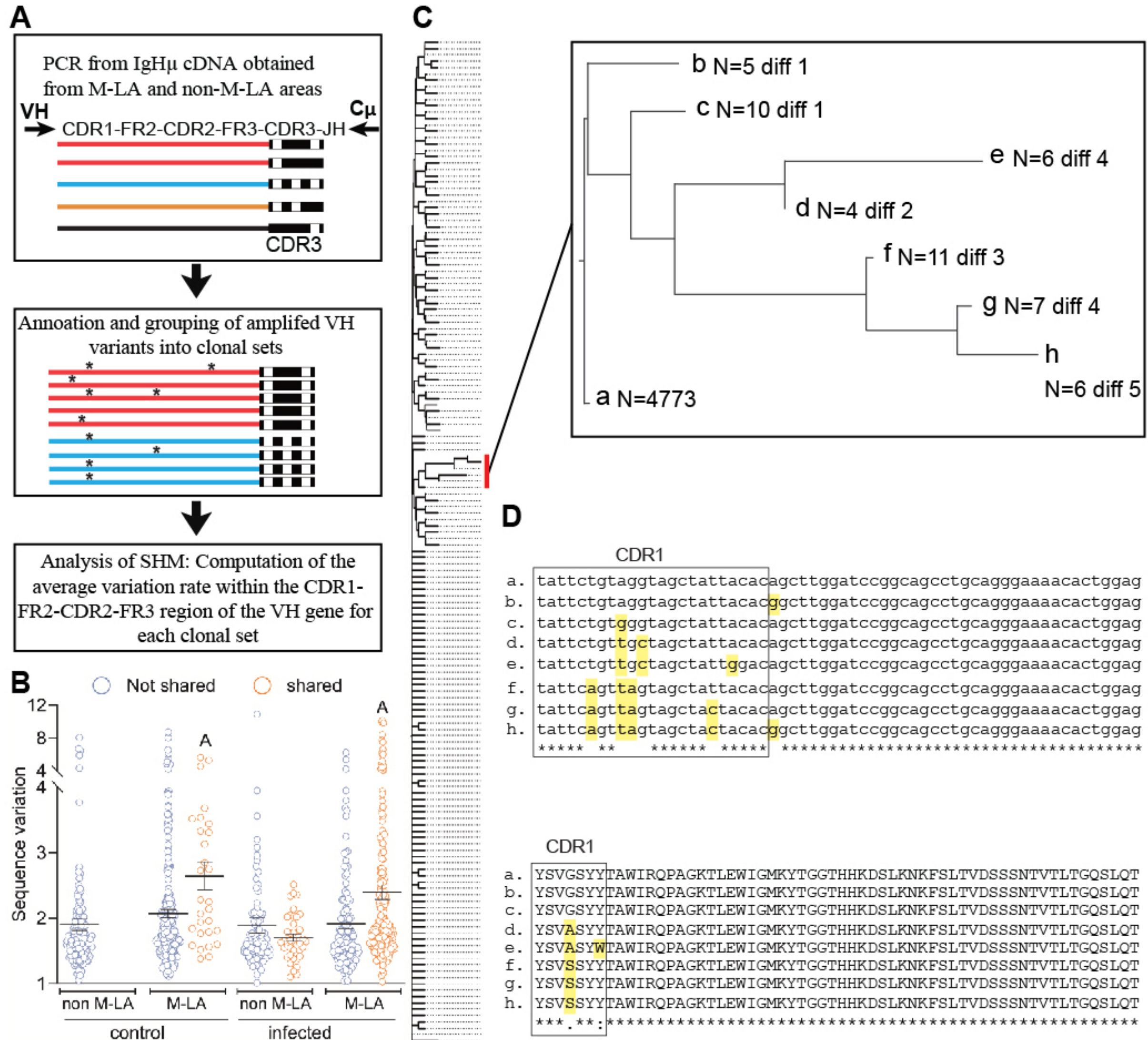

Fig. 7. IgHμ V gene sequences are somatically hypermutated prevalently in clonal sets shared among M-LAs from the same spleen. (**A**) Pipeline of analysis of sequence variation within clonal sets from M-LA and non M-LA areas of control and infected fish. (Clonal sets are defined as sets of sequences with the same CDR3 and the same VH gene annotation). Different color lines in upper panel denote different VH genes. Black rectangles at the end of each line represent the VDJ junction while the different number and/or position of the white squares within them denote sequence differences in the VDJ

junction. In the middle panel, two different clonal sets (one in read and the other in blue lines respectively) are represented. Asterisks denote sequence differences of individual VH variants within each clonal set. (**B**) Sequence variation was calculated for shared and non-shared clonal sets from M-LAs and non M-LA areas of the same spleen from control
5 ($n = 4$) and infected fish ($n = 3$). Variation is represented as the proportion (per 1000) of nucleotides divergent from the most frequent sequence of the clonal set. Horizontal lines represent mean (± SEM), empty circles represent the sequence variation value found in a clonal set. Scatter groups with the letter A above are significantly different with the other groups (two-way ANOVA, Tukey test, $P < 0.05$). (**C**) Example of a tree of sequences of a
10 clonal set from an M-LA of an infected fish (this clonal set is defined by the expression of the IGHV6-4 gene and its CDR3 sequence). This clonal set comprised 9174 sequences (representing 1102 unique sequence variants). The Neighbor Joining tree was computed by Clustal Omega, and comprises all sequences found more than 5 times (i.e., 309 sequence variants). A magnification of a tree branch showing accumulation of mutations
15 is shown on the right. "N" is the number of sequences found in the dataset for each variant, while "diff" refers to the number of nucleotide differences to the reference sequence (sequence "a" of panel D). (**D**) Multiple alignment of nucleotide and amino acid sequences of tree branch shown in C. Mutations are highlighted in yellow. The CDR1 is boxed.

Supplementary Materials for

Cold-blooded vertebrates evolved organized germinal center like structures

5 Yasuhiro Shibasaki[1,2]§, Sergei Afanasyev[3]†, Alvaro Fernández-Montero[1]†, Yang Ding[1], Shota Watanabe[2], Fumio Takizawa[1,4], Jesús Lamas[5], Francisco Fontenla[6], José Manuel Leiro[7], Aleksei Krasnov[8]‡, Pierre Boudinot[9]‡, J. Oriol Sunyer[1]*

*Correspondence to: sunyer@vet.upenn.edu (J.O.S.)

‡Equal secondary corresponding author. Email: pierre.boudinot@inrae.fr (P.B.)

10 Aleksei.Krasnov@nofima.no (A.K.)

This PDF file includes:

Materials and Methods

Fig.S1-S6

15 Table S1-S2

MATERIALS AND METHODS

cDNA synthesis, RT-PCR and Illumina sequencing of IgHμ CDR3s repertoire

To analyze the expressed IgHμ CDR3 repertoire from laser capture microdissected M-LAs and non M-LA areas from the spleen of Ich reinfected fish, DNP-KLH boosted fish, and the respective control fish, we specifically amplified IgHμ cDNA transcripts from the total RNA preparations obtained from each microdissected area as described above. To this end, first strand cDNA was synthesized using 10 to 20 pg of total RNA with Superscript IV reverse transcriptase (Thermo Fisher Scientific) using the IGMR1 primer (table S1). For IgHμ CDR3 analysis, the first strand cDNA was amplified with IGV5 (table S1) and IGC3 primers (table S1) using Platinum Hot Start PCR Master Mix (Thermo Fisher Scientific) for 30 cycles. These PCR products therefore contained the end of the frame region 3 (FR3), the CDR3 and the IGHJ segment of IgHμ. Illumina adaptors were then introduced in a second PCR (10 cycles) using Nextera™ XT Index Kit v2 (Illumina). These PCR products were measured with Qubit (Thermofisher Scientific), were combined and purified twice with Qiagen PCR clean up kit. These libraries were then sequenced with MiSeq™ Reagent Kits v3 (Illumina) (150 cycles) according to manufacturer's instructions. CDR3-IMGT sequences (positions 105 to 117 in IMGT numbering [*i.e.,* position following the Cys$_{104}$ to position preceding J-TRP$_{118}$ in IgHμ sequences]) from each sample were extracted and organized in a database.

Analysis of somatic hypermutation (SHM)

To look for evidence of SHM in IgHμ V sequences, we amplified the IgVHμ region containing CDR1-FR2-CDR2-FR3-CDR3-IGHJ, using as template the IgHμ cDNAs from the same M-LA and non M-LA areas obtained in the previous section (CDR3 repertoire analysis). To this end, we used a forward VH-specific primer cocktail (table S1) covering all IGHV subgroups while

Cμ1_R (primer in the first constant domain of IgHμ) was used as a reverse primer (table S1). After amplification, Miseq Illumina libraries were constructed from these amplified PCR products, and sequenced as described in the above section using MiSeq™ Reagent Kits v3 (Illumina). The obtained sequences were analyzed by IMGT/HighV-QUEST, based on our rainbow trout annotation of the IgH locus (*50, 51*). IGHV gene annotation proposed by IMGT HighV-QUEST was validated when the sequences were > 97.5% identical to the closest germline sequence in the aforementioned IMGT database. The non-validated sequences (i.e., gene/allele variation) were discarded to reduce the probability of confusion between sequence variation due to hypermutation detected in the validated sequences and that derived from gene/allele variation arisen during evolution. Among sequences kept for further analysis (i.e., validated sequences), those with identical CDR3-IMGT (i.e., sequences with the same nucleotide sequence encoding residues 105 to 117, between conserved Cys_{104} and TRP_{118} of the V domain), and with the same IGHV gene annotation, were grouped thus becoming a "clonal set" (as described in (*52*)) . Within each clonal set, reads that deviated by more than five nucleotides from the most frequent sequence of the clonal set were filtered out, again to reduce the risk of including divergent germline variants produced during evolution. This highly conservative approach for producing sequence lineages excluded both SHM located in the CDR3 as well as potential heavily mutated sequences, but it offers a maximum guarantee of avoiding variations due to illicit grouping of related distinct genes. Sequence variation (i.e., SHM) was assessed within each clonal set containing more than 30 sequences and was computed as the number of nucleotides deviating from the most frequent sequence of the clonal set divided by the total number of nucleotides. Sequence variation was computed both in shared and non-shared clonal sets of M-LAs or non M-LA areas within the spleen of the same fish. Sharing of clonal sets in different M-LAs or non M-

LA areas was defined as the presence in these areas of at least one sequence of the clonal set (i.e., if 3 M-LAs were obtained from the same spleen, a clonal set was considered shared when at least one of its sequences was identified in each of the 3 M-LAs). In contrast to these shared clonal sets, we considered non-shared clonal sets in which their sequence variants could only be found in one of either the M-LA or non M-LA areas of the same spleen.

Immunofluorescence microscopy

Spleen tissues were sampled and embedded in Tissue-Tek OCT compound (Sakura Finetek). Spleen cryoblocks were sectioned at a thickness of 5 μm and then fixed for 10 min in 4% paraformaldehyde (PFA; Wako Chemicals). For the detection of trout IgM^+ B cells and $CD4^+$ T cells, tissue cryosections were immunostained as previously described by us (*19, 49*). Briefly, we used mouse anti-trout IgM monoclonal antibody (mAb) (clone: 1.14, mouse IgG1; 1 μg/ml) (*53*) and affinity purified guinea pig (gp) anti-trout CD4 polyclonal antibody (pAb) (1 μg/ml) to incubate the cryosections overnight at 4 °C. For the detection of cells expressing activated caspase 3, a rabbit anti-human caspase 3 (ab13847-100; 1:300 dilution; Abcam) which cross-reacts with several species, including rainbow trout, was used following the methodology described in (*29*). As antibody controls for anti-trout IgM mAb, anti-trout CD4 pAb, and anti-human caspase 3, we used mouse IgG1 (clone MOPC-21, Biolegend), guinea pig IgG purified from pre-immune sera and rabbit IgG isotype control (Invitrogen), respectively. To detect anti-trout IgM mAb, anti-trout CD4 pAb, and anti-human caspase 3, cryosections were incubated for 2 h at room temperature (RT) with Alexa Fluor 488-conjugated goat anti-mouse IgG1 (Invitrogen), Alexa Fluor 568-conjugated goat anti-guinea pig IgG (Invitrogen) and Alexa Fluor 647-conjugated goat anti-rabbit IgG (Invitrogen) respectively at 2.5 μg/ml each. Cell nuclei were stained with DAPI (1 μg/ml; Sigma-Aldrich) and the slides were mounted with Fluoroshield

(Abcam). Images were acquired by using a Leica DM6000 fluorescence microscope at the Penn Vet Imaging Core (the University of Pennsylvania), or a Leica SP8 confocal microscope at General Research Institute (Nihon University) and analyzed with LAS X software. When required, the area of images was measured by ImageJ as described in (*54*). IgM^{hi} and IgM^{low} B cells were analyzed using LAS X software (IgM positively stained cells were determined as IgM^{hi} cells when cells exhibit saturated signal using the the Over /Underexposure mode).

Proliferation of IgM^+ B cells and $CD4^+$ T cells on cryosections was performed as previously reported by us in (*19, 49*). Briefly, fish were anesthetized with MS-222 (100 mg/l) and i.p. injected with 200 µg of 5-ethynyl-2'-deoxyuridine (EdU; Invitrogen) in 100 µl of PBS. After 24 h, animals were euthanized as described above, and spleen organs were harvested and embedded in Tissue-Tek OCT compound (Sakura Finetek). The cryoblocks were sectioned at a thickness of 5 µm and then fixed for 10 min in 4% PFA. EdU^+ cells were stained with Click-iT EdU Alexa Fluor 647 Imaging Kit (Invitrogen) according to the manufacturer's instructions. EdU-stained spleen cryosections were then stained with anti-trout IgM mAb and anti-trout CD4 pAb as described above to detect IgM^+ B cells and $CD4^+$ T cells, respectively. Cell nuclei were stained with DAPI (1 µg/ml) before mounting with Fluoroshield. Images were acquired and analyzed using a Leica DM6000 fluorescence microscope or Leica SP8 confocal microscope and LAS X software.

Quantification of cells on tissue sections

To quantify the number of proliferating cells or other cell types in splenic MMCs and non-MMC areas, we adapted a methodology used to count cells in GCs reported in (*55, 56*). Briefly, images from stained spleen sections were acquired by using a Leica DM6000 fluorescence microscope at the Penn Vet Imaging Core (the University of Pennsylvania), or a Leica SP8 confocal

microscope at General Research Institute (Nihon University). On these images, the exact perimeter containing aggregates of proliferating cells within and nearby a given MMC was first drawn using Fiji ImageJ software (*57*), and proliferating cells within that perimeter were then counted using the same software. To normalize the number of proliferating cells per area of
5 tissue, number of proliferating cells were expressed per 0.1 mm^2. To count proliferating cells in non-MMC areas of the same spleen section, we counted proliferating cells within non-MMC areas equivalent in size to those counted for MMCs. For instance, if for one spleen section we counted proliferating cells in 3 different MMC areas (each measuring 0.2, 0.1 and 0.3 mm^2 respectively), we then counted proliferating cells in 3 different non-MMC regions containing the
10 same areas of those measured for MMCs (0.2, 0.1 and 0.3 mm^2). The aforementioned approach was also used to count the number of IgM^{hi}, IgM^{low} cells in splenic MMCs and non-MMC areas, as well as the number of proliferating B and T cells in splenic M-LAs and non-M-LA areas from control and infected fish.

15 *In situ hybridization*

An 820-bp fragment of trout AID cDNA (GenBank accession number: XM_036961711.1) and a 1742-bp fragment of the constant region of trout IgM heavy chain cDNA (GenBank accession number: S63348.1) were subcloned into pGEM-T easy vector (Promega) according to the manufacturer's instructions. The AID probes (table S2) were synthesized using DIG RNA
20 Labeling Kit (Roche) and the IgM heavy chain probes (table S2) were synthesized using biotin RNA labeling Mix (Roche) and stained following the manufacturer's instructions. Spleen cryoblocks were sectioned at a thickness of 10 µm and then fixed for 2 h at 4 °C in 4% PFA, and washed three times with PBS. The sections were permeabilized by incubating in 0.5% PBS-Tween for 15 min at RT and then acetylated . Following acetylation, the sections were washed

with PBS and then prehybridization was carried out in hybridization solution (4× saline sodium citrate buffer [SSC; Corning Life Sciences], 40% formamide [WAKO], 10% dextran sulfate sodium [WAKO], 2× Denhardt's solution [WAKO], 0.5 mg/ml yeast tRNA [Thermo fisher], 1× RNase inhibitor [Sigma-Aldrich]) for 10 min at RT. Hybridization was performed with DIG-labeled and biotinylated RNA probes (final concentration, 1.1 μg/ml) in hybridization solution for 18 h at 50 °C in a humidified chamber. After hybridization, the slides were washed as follows: 2× SSC for 5 min at RT, 2× SSC containing 10% formamide for 20 min at 50 °C, twice with 1× SSC for 30 min at 50 °C, and PBS for 10 min at RT. Prior to immunostaining, the slides were blocked with 2% PBS-BSA. Anti-Digoxigenin-AP, Fab fragments (Roche) at a dilution of 1:250 and Streptavidin Alexa Fluor 488 (Biolegend) with blocking solution were applied and incubated overnight at 4 °C. Subsequently, the slides were washed three times for 5 min with 0.05% PBS-Tween at RT and finally for 5 min in PBS at RT. Hybridized signals were visualized using ImmPACT Vector Red AP Substrate kit (Vector Laboratories). Cell nuclei were stained with DAPI (1 μg/ml) before mounting with Fluoroshield and images were acquired and analyzed using a Leica DM6000 fluorescence microscope or Leica SP8 confocal microscope and LAS X software.

Analysis of trout DNP-KLH-specific IgM titers by ELISA

DNP-KLH or KLH (Millipore) were used as the antigen for coating the ELISA plates. Antigen (20 μg/ml in 0.05M carbonate-bicarbonate buffer, pH9.6; 50 μl per well) was absorbed overnight at 4 °C onto MICROLON microplates (Greiner). Nonspecific binding sites were then blocked with 8% skim milk in PBS. Plates were washed with 0.05% PBS-Tween. Serum samples from control or DNP-KLH immunized fish were serially diluted in PBS. For analysis of the binding of IgM to antigens, biotinylated anti-trout IgM (0.5 μg/ml in 1% PBS-BSA) was added

to each well. After 2 h of incubation at RT, plates were washed and bound antibodies were detected by incubation with Pierce High Sensitivity Streptavidin-HRP (0.5 µg/ml; Thermo Fisher Scientific), followed by color development with TMB ELISA Substrate (Abcam) as a substrate. After 30 min, the color reaction was stopped with a solution of 0.6 N sulfuric acid and absorbance was measured at 450 nm by microplate reader (InfiniteF50 Plus, TECAN). DNP-specific antibody endpoint titers are presented as the reciprocal of the highest serum dilution that provided an average absorbance exceeding twofold the average background absorbance at 405 nm.

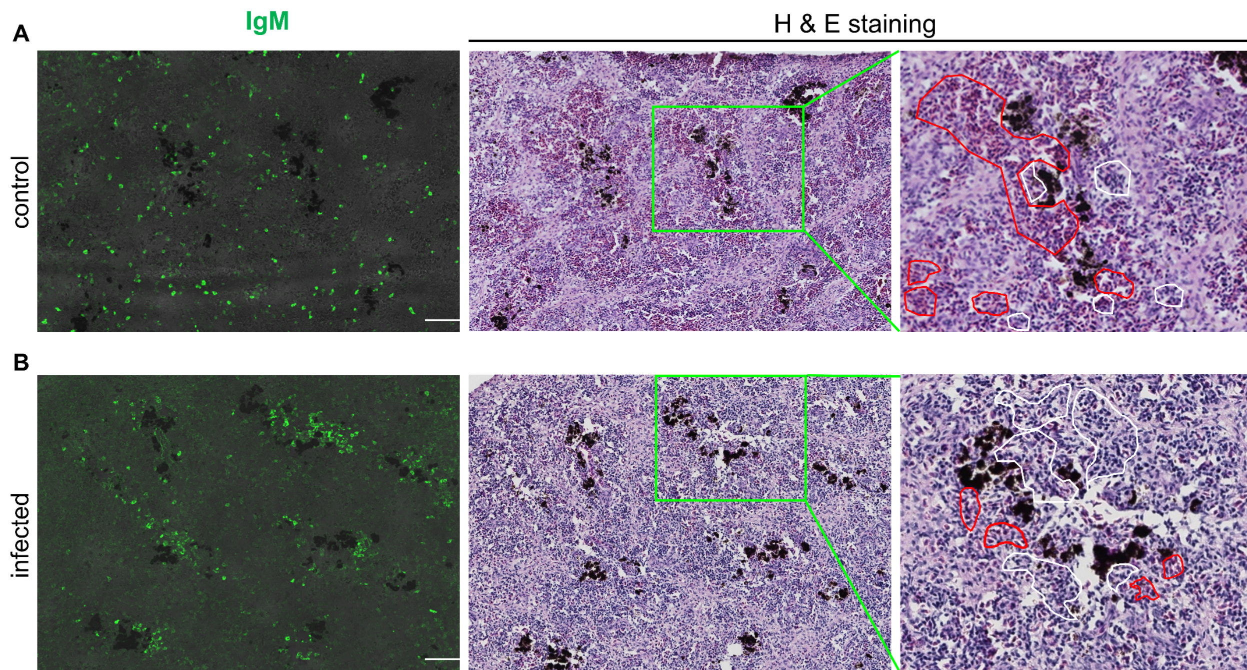

Fig.S1 Red and white pulp from spleen of control and infected fish. (**A** and **B**) Histological analysis of spleen from control (A) and infected (B) fish. Spleen cryosections were first stained for IgM (green), followed by H&E staining. Right panels of (A and B) show enlarged images of the areas outlined in middle panels, each containing an MMC and its surrounding tissue. White and red lines in right panels of A and B outline representative areas of white and red pulp respectively. As seen in these images, red and white pulp of trout spleen intermingle throughout the spleen.

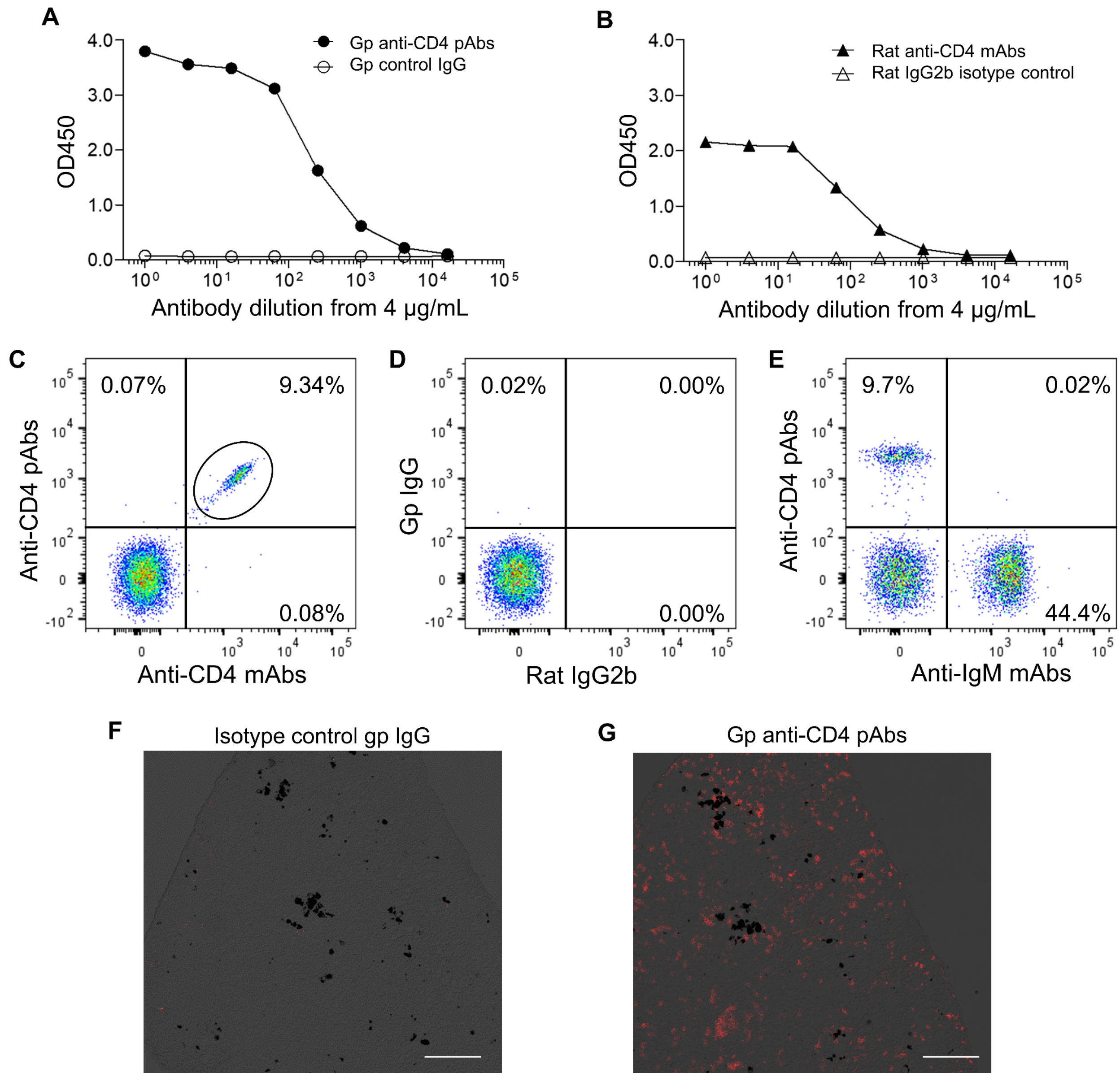

Fig.S2 Validation of a newly developed guinea pig anti-trout CD4 pAb reagent. (**A** and **B**) Representative ELISA showing the reactivity of guinea pig (gp) anti-trout CD4 pAb (A) and rat

5 anti-trout CD4 mAb (B) against recombinant trout CD4. ELISA plates were coated with recombinant trout CD4 which was detected with gp anti-trout CD4 pAb (A) or rat anti-trout CD4 mAb (B**)** or their respective isotype control Abs (gp IgG and rat IgG2b). (**C** to **E**) Flow

cytometry of trout splenic leukocytes double-stained with: gp anti-trout CD4 pAb and rat anti-trout CD4 mAb (C), isotype control for gp IgG and rat IgG2b (D), and gp anti-CD4 pAb and mouse anti-trout IgM mAb (E). (**C** to **E**) show representative dot plots of the lymphocyte gate. Numbers in quadrants in each dot plot represent percentage of positively stained cells. (**F** and **G**) Immunofluorescence analysis of spleen from a naïve fish. Consecutive cryosections were stained with isotype gp IgG (F) or gp anti-trout CD4 pAb (G). Data are representative of at least three independent experiments (n = 3-4 fish/experiment). Results show that gp anti-CD4 pAb (A) recognizes recombinant trout CD4 to a higher degree than the rat anti-CD4 mAb (B). Moreover, gp anti-trout CD4 pAb and rat anti-trout CD4 mAb double-stain the same $CD4^+$ T cells (black circle in(C)) thus indicating the correct specificity of the gp anti-trout CD4 pAb. As expected, this new gp anti-trout CD4 pAb did not cross-react with IgM^+ B cells (E). Isotype control gp IgG did not produce any significant staining (D and F).

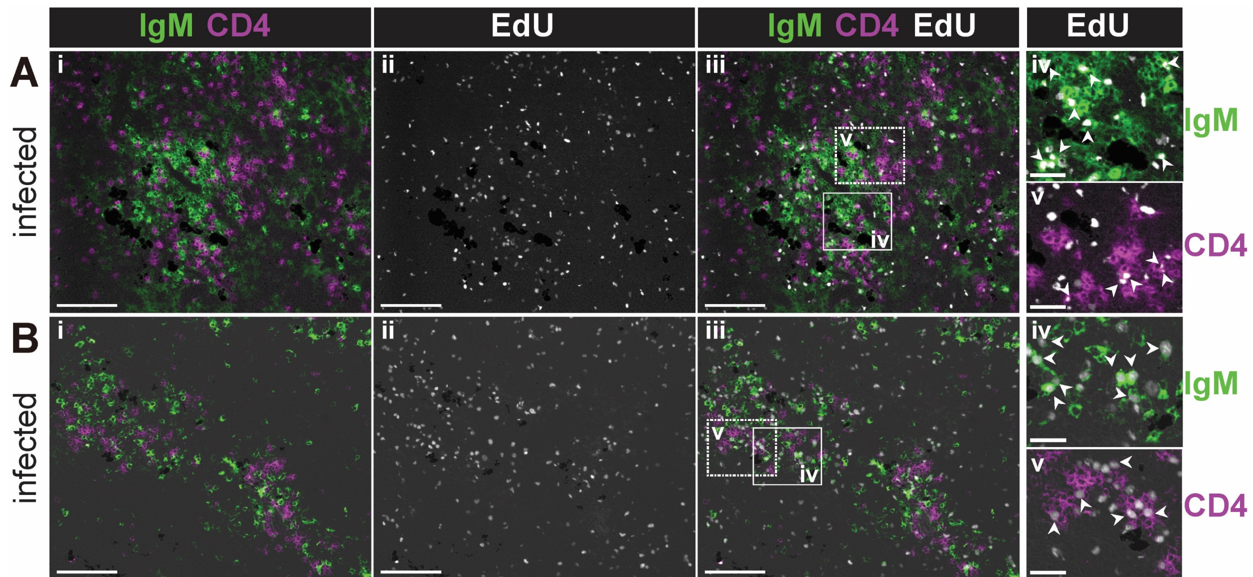

Fig.S3 Boundaries between B and T cell aggregates are not clear in some M-LAs from infected fish. (**A** and **B**) Immunofluorescence analysis of EdU incorporation by IgM$^+$ B cells and

5 CD4$^+$ T cells from M-LAs of spleen of infected. Spleen cryosections were stained for IgM (green), CD4 (magenta), EdU (white). Image in (i) shows a representative M-LA stained for IgM (green) and CD4 (magenta); (ii and iii) show the same tissue area of (i) stained for EdU (white) (ii), IgM (green), CD4 (magenta) and EdU (white) (iii); (iv and v) show enlarged images of the areas outlined in (iii) displaying proliferating (EdU$^+$) IgM$^+$ B cells (iv) and proliferating (EdU$^+$)

10 CD4$^+$ T cells (v). White arrowheads point to examples of proliferating IgM$^+$ B cells (iv) and CD4$^+$ T cells (v). Scale bars, 100 µm (i to iii), and 20 µm (iv and v). Groups of dark cells in all images represent MMCs. Data is representative of at least three independent experiments.

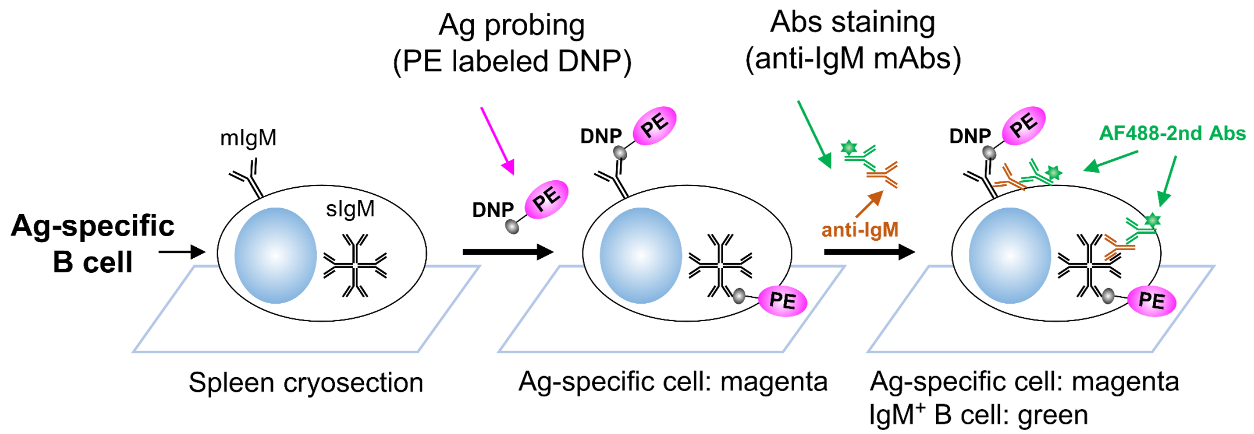

Fig.S4 Detection of antigen(Ag)-specific B cells on spleen cryosections. Scheme of the strategy used to detect Ag-specific B cells on spleen cryosections from control or immunized fish. Cryosections were first stained with the antigen probe (DNP-PE), followed by anti-trout IgM mAb and anti-trout CD4 pAb and their corresponding secondary Abs. The cryosections were analyzed by confocal microscopy. mIgM: Membrane IgM; sIgM: Secreted IgM.

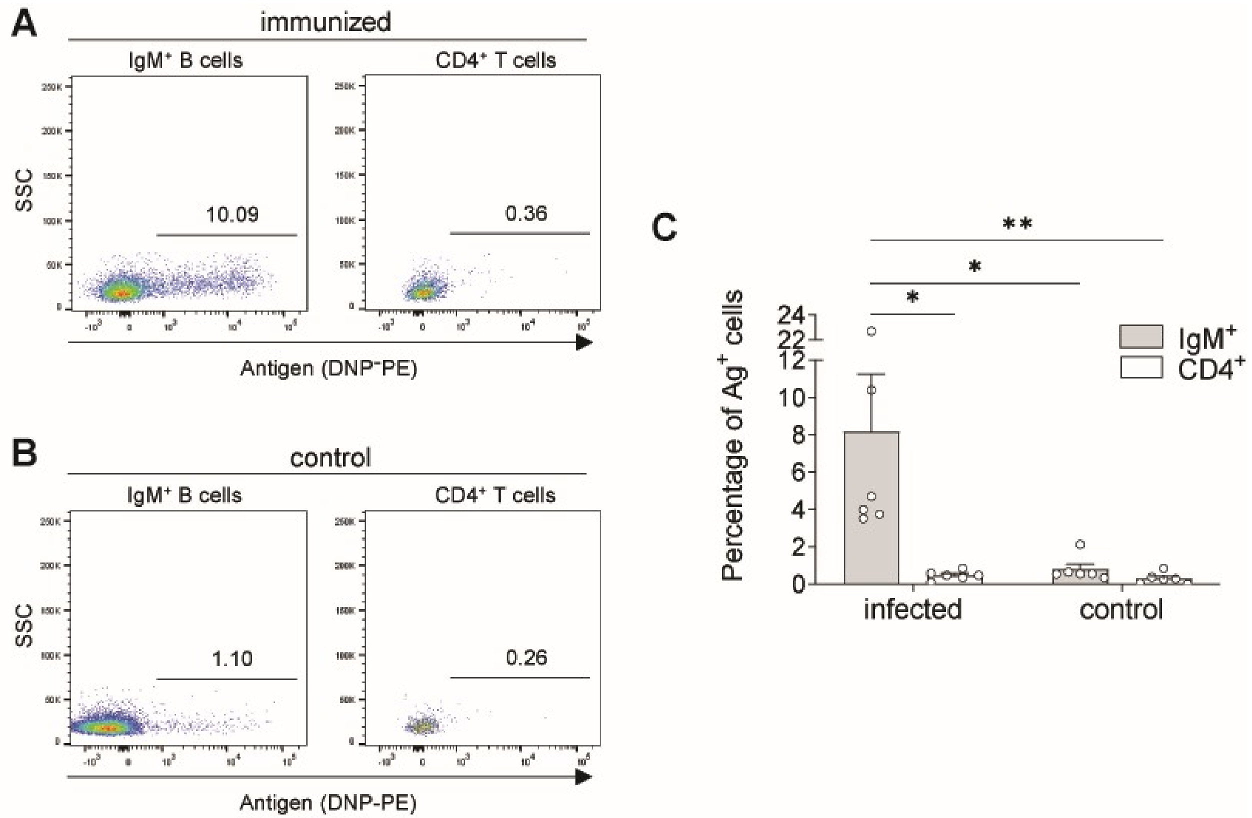

Fig.S5 Detection of antigen-specific B cells by flow cytometric analysis. Leukocytes from the spleen of control or DNP-KLH immunized fish were co-stained with the antigen probe (DNP-PE) and the anti-trout IgM mAb or anti-trout CD4 pAb and their corresponding secondary Abs. (**A** and **B**) Representative dot plots showing the binding of DNP-PE to IgM$^+$ B cells (left) and CD4$^+$ T cells (right) from immunized fish (A) or control fish (B). (**C**) Percentage of IgM$^+$ B cells and CD4$^+$ T cells binding DNP-PE. (**A** to **C**) 6 immunized and 6 control fish were analyzed. Empty cycles represent values from individual fish. Statistical analyses were performed by two-way ANOVA followed by Tukey's test. *P < 0.05, **P < 0.01.

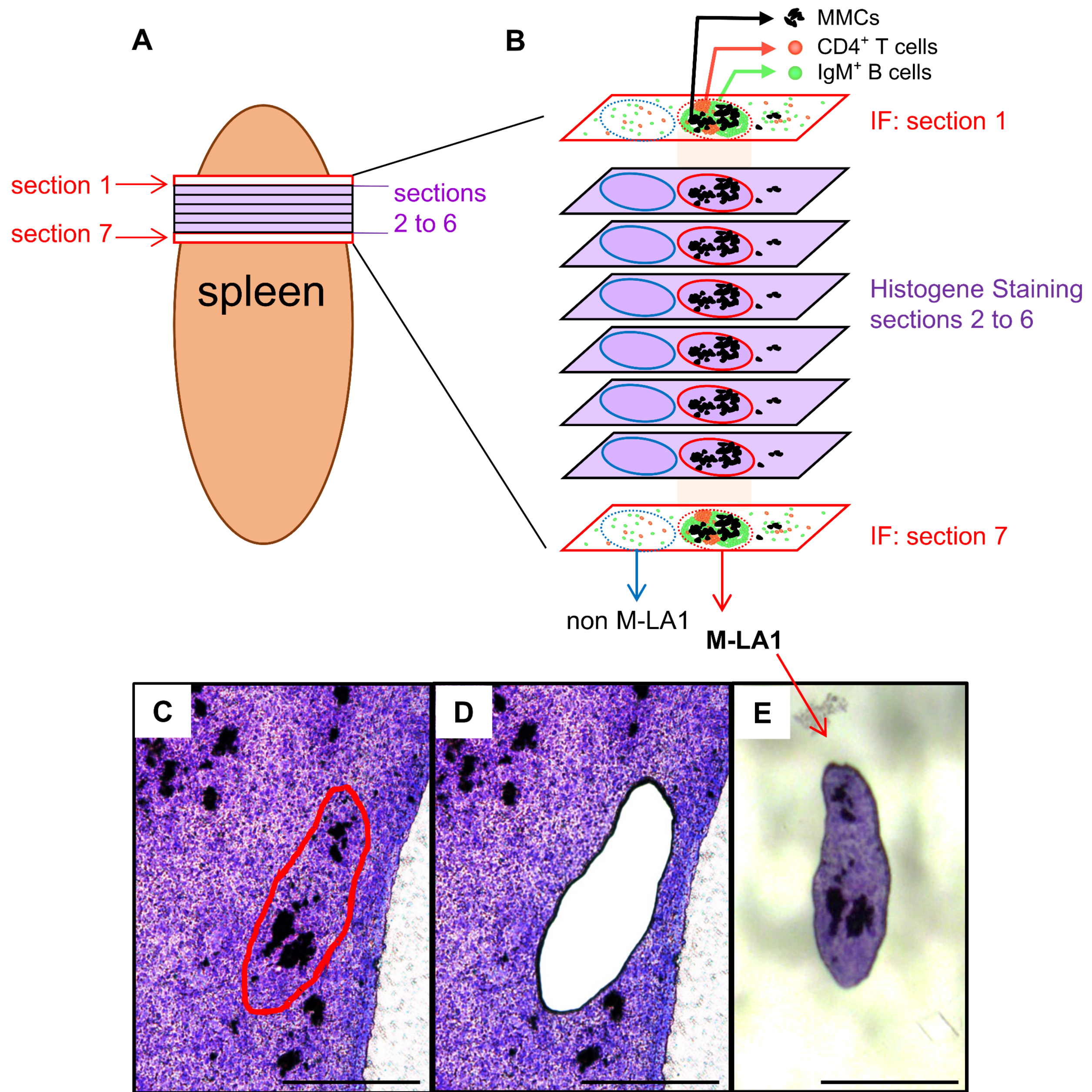

Fig.S6 Strategy to harvest splenic M-LA and non M-LA areas by laser capture microdissection (LCM). (**A**) To identify M-LA and non M-LA areas from sections of the same spleen, a first section (top red) from the spleen is stained for IgM, CD4 and EdU as described in
5 (Fig. 2) with the goal to identifying M-LAs and non M-LA areas. Once identified, five consecutive sections are then obtained and the seventh section (bottom red) is stained again with

the same Abs to confirm that the M-LA is still in that region and that the chosen non M-LA areas remain devoid of M-LAs. This process may be repeated several times in these same areas, depending on the thickness of that specific M-LA or non M-LA area (B shows a graphic representation of a spleen section depicting an M-LA and a non M-LA area [black areas of the
5 section represent MMCs]). (**C**) To microdissect M-LA and non M-LA areas from the non-stained spleen sections (sections 1 to 5 of B), that section is first stained with snap H&E staining (Histogene Staining Solution) for easy identification of melanomacrophages (dark cells). As an example, we show the laser capture microdissection of an M-LA from a snap H&E-stained section (C to E). Using the Leica software from the LCM apparatus we can quantify the exact
10 area of the M-LA that has been microdissected, and these data is then used to harvest the same amount of area from a non M-LA region of the same spleen. Scale bar, 200µm.

Supplementary Table 1. Primer sequences used in this study.

Primer	Sequences (5'-3')	Used for
IGMR1	TAAAGAGACGGGTGCTGCAG	First strand cDNA synthesis
IGV5	TGARGACWCWGCWGTGTATTAYTGTG	Analysis of IgHμ CDR3 diversity
IGC3	GGAACAAAGTCGGAGCAGTTGATGA	
Forward VH-specific primer cocktail:		Cocktail primers used for hypermutation analysis
IGHV1-10_F	ACTAACTGAGTCTGGGCCAG	
IGHV1_F	ATTGACKGAGTCTGGAYCAK	
IGHV2_F	ACTMTMAGTCTSTCCTGTAAG	
IGHV3_F	TGCAGCCTGGACAGCCTCTGAC	
IGHV4_F	GGATCAGTCWCCTYCTCARGTG	
IGHV6_F	GACTGTCCWGCCAGGTCAACC	
IGHV7_F	GTAAAGCCTGGAGAGTCTCTG	
IGHV8_F	AAACTCACATGTGCCTGTAGTG	
IGHV9_F	GAGTCAGTAACASTGTCMTGT	
IGHV10_F	CCAGGAGAGTCTKTCASCATC	
IGHV11_F	GTGAAACTATCTTGCCAAGT	
IGHV12_F	CTTTGAGCATCACCTGTAAGG	
IGHV14_F	TTGACTATCAGTTGTGCAATC	
IGHV15_F	AGAAACTCTCAAYCTMTCYTG	
IGHV16_F	CTCAGCCTCTCCTGTAAGGGA	
Cμ1_R	CACATTGCGCAAGAGGGAACAA	Reverse primer used for hypermutation analysis

5

Supplementary Table 2. Probe sequences used in *in situ* hybridization.

Gene	Used for	Sequences (5'-3')
Aid	anti-sense	TCACAGTCCAAGTAGCTCAAAAGCATCTCCCCAATCTTCTGCCTCACCAGGCTGGAGGATGTCGTT AAGTTTCCTGGCCAGTTGAACAGAGTTCTGATGCAGTCCGTCCCAGGCCTTAAACACACGCTGTCT GCAAGCTACAAAGGTCTGCCAACAGTAGAAATAGTCTTCATAGTTCATGACAGTGATCTGCACCC CGGCTCTCTGCAGCATGCGGAGACCCTCTCTCGCACTGCTGTCCTCCGGGTCACAGAAGTAGAGC CTGGAGACATAGATCCTGAGGCGGAGGTTGGGGGTCTGGCTGAGGAACTGGGCCAGCCTGTAGG AGCAGTCTGAGCAGGGGGACCAGGAACAGAACCAGGTGACTGAGTAACACAGTCCCACACTGTC TGGAGCTCCATAACCCCACAGGCCTGGACACAGGGCGCCTGCTTCCAGGAGGCGCAGGAACAGC AGCTCAACATGACAGCCGGACCGGTTGCGCAGGTGTCCAAAGTCGAAGGAGAGTGAGTTTGGTCC CACCCGCCTCTTGACCACAAAGCACAGGTAGGTTTCGTGTCGGCCCTTGGCCCAGCGCATGTTCTT ATAGTGGTAGATAAACTTCTTCTGGGCCAACAGAACACTGTCAAATTTGTTGATCAT
	sense probe (control probe)	ATGATCAACAAATTTGACAGTGTTCTGTTGGCCCAGAAGAAGTTTATCTACCACTATAAGAACAT GCGCTGGGCCAAGGGCCGACACGAAACCTACCTGTGCTTTGTGGTCAAGAGGCGGGTGGGACCA AACTCACTCTCCTTCGACTTTGGACACCTGCGCAACCGGTCCGGCTGTCATGTTGAGCTGCTGTTC CTGCGCCTCCTGGAAGCAGGCGCCCTGTGTCCAGGCCTGTGGGGTTATGGAGCTCCAGACAGTGT GGGACTGTGTTACTCAGTCACCTGGTTCTGTTCCTGGTCCCCCTGCTCAGACTGCTCCTACAGGCT GGCCCAGTTCCTCAGCCAGACCCCCAACCTCCGCCTCAGGATCTATGTCTCCAGGCTCTACTTCTG TGACCCGGAGGACAGCAGTGCGAGAGAGGGTCTCCGCATGCTGCAGAGAGCCGGGGTGCAGATC ACTGTCATGAACTATGAAGACTATTTCTACTGTTGGCAGACCTTTGTAGCTTGCAGACAGCGTGTG TTTAAGGCCTGGGACGGACTGCATCAGAACTCTGTTCAACTGGCCAGGAAACTTAACGACATCCT CCAGCCTGGTGAGGCAGAAGATTGGGGAGATGCTTTTGAGCTACTTGGACTGTGA

Igmµ heavy chain	anti-sense probe	GGCCGCGAATTCACTAGTGATTATGCATCTCTGAGGCACATTCAAGCTGAGGTTAACTAGGTTGG GTTGGTTTGAGGTTCTGTCAATGGTTCTCATAAGAATTTTTGTGGACTTGATCATGCTTTCGTGGTA AACTACACAGCTATAGACCACTTCTTCGTTCTTCCACAAGTCATTGCTAAATGTGAGCTGACTGTA GACAGAGTANGTCCTTCCTGATTGAATCTGGCTAGTGGTGTTGAATTGGTACAATGCTGAACTGCT CGTTCTCTCCACCGGCTCATCGTCAACAAGCCAAGCCACTAAAACGTCCTTGGGGTAGAAATCTTT GACGTACCAAGTCAGGGTCACCGTATTATCACTAGTTTGTTCTGCTGGAGCCAGCAGAAAGACAG ATGGACGCTGTGGAACTCCTCCGGTCTCCCTCTTGTAGGCTTTCTTTACCAAGTCCCCCAGGTTTTC CATGTGATCTACAGCGCAGTAGAATACTGTCCCATTGCTCCAGTCCTCATAAGTGATGTCAAGTAT GGCAATTTTGTCAGTGACACCCTTTCGGCTGGTTAAGGTCTTTCCATTGTCATTTTCCCATTTGACG CTCAGGAAGCCAGGAACTAGTTCATTGACATCACACACAAGCTGCGCTTTTTTGTTCATAAGCATA TCCTCAAGAGACGGCTCGATGATCGTAATGACTACTGAATGTCCATGGACTGGACCATCTGATGA AGTGTAGCCCACAGTTCTCCTCACATTTCCAGCTTTGTTCTCAAACACGCAAGTGAATGTTACTTC TTCACTCTTCCACTCACTCTCATTGACTCTGAGATAGCTGGTTGTGCTGTACAGAGTTGTCTCACTC TTCTTCTCACTCTCACAARAACTCTTGAAATCAGATACAACTTCTTGTTCTGTTCCTTTTTCCATCCT CATCCATTTGATTGTGTGTGTACGGGGTGAAAAGTCATTGGCAAAGCAGGCGAAGGAAGCCGTCT TATTTTCTGACATCTCCTCTTTASAGGGGGTCATTACGTAAAGAGACGGCTGCTGCAGATATTCCG GTTGTTTTTTCACTGGTACTTTCTTTGATCCAGCAGAATGTTCCACGGCGCACTCAAATTTTTTACT GTCCCAGTCTGCTCTCTTTACACGGAGTTGACTGACTCCCATGTARCTTCCACCGGTTTGGACCGC AGGGTACTGAACGAAATCARTCAGGGAATTCCCGCCTTCGTCATTCCATTTGAAGGTGAGGGAGG CAGGCGTGAAGCCAGTGGCAATGCAACCCAGAGTCATCATATCTCCGGTCCCGGAGCCACATTGC GCAAGAGGGAACAAAGTCGGACCAGTTGAWGAGGSTGTGGACACGGTCACCATGGTCCCTTTCC CCCAGTAGTCAAAGTAGTTGTAGCTCCCAGTGTATCTGGCACAATAATACACAGCAGAGTCTTCA GTTTTCAGGCTGTTCATCTGGAGATACACCTGCTTCATGATGTTGTGTCTGGAGATGGTGAACCGA CCTTGAACAGACTGAGAGTAGGCAATATTTCTAATGTCATAATGCGCTGCCACAAATTNTAGTCCT

		TTACCAGGAGCCTGTATGATCCATGCAATCCAATAGCCATTTATGTTCAAATTAGAGGCAGTACA GGTCAGTTTGTGGGTTTNTAAAGGCTTTTTAACCATTGGTCCAGACTCAGTCAGTTTTTGACTATG AACACCTATCAGTCTTATTATCATCAGTAAAAACACAGTAGTAAATGAATC
	sense probe (control probe)	GATTCATTTACTACTGTGTTTTTACTGATGATAATAAGACTGATAGGTGTTCATAGTCAAAAACTG ACTGAGTCTGGACCAATGGTTAAAAAGCCTTTANAAACCCACAAACTGACCTGTACTGCCTCTAA TTTGAACATAAATGGCTATTGGATTGCATGGATCATACAGGCTCCTGGTAAAGGACTANAATTTGT GGCAGCGCATTATGACATTAGAAATATTGCCTACTCTCAGTCTGTTCAAGGTCGGTTCACCATCTC CAGACACAACATCATGAAGCAGGTGTATCTCCAGATGAACAGCCTGAAAACTGAAGACTCTGCTG TGTATTATTGTGCCAGATACACTGGGAGCTACAACTACTTTGACTACTGGGGGAAAGGGACCATG GTGACCGTGTCCACASCCTCWTCAACTGGTCCGACTTTGTTCCCTCTTGCGCAATGTGGCTCCGGG ACCGGAGATATGATGACTCTGGGTTGCATTGCCACTGGCTTCACGCCTGCCTCCCTCACCTTCAAA TGGAATGACGAAGGCGGGAATTCCCTGAYTGATTTCGTTCAGTACCCTGCGGTCCAAACCGGTGG AAGYTACATGGGAGTCAGTCAACTCCGTGTAAAGAGAGCAGACTGGGACAGTAAAAAATTTGAG TGCGCCGTGGAACATTCTGCTGGATCAAAGAAAGTACCAGTGAAAAAACAACCGGAATATCTGCA GCAGCCGTCTCTTTACGTAATGACCCCCTSTAAAGAGGAGATGTCAGAAAATAAGACGGCTTCCTT CGCCTGCTTTGCCAATGACTTTTCACCCCGTACACACACAATCAAATGGATGAGGATGGAAAAAG GAACAGAACAAGAAGTTGTATCTGATTTCAAGAGTTYTTGTGAGAGTGAGAAGAAGAGTGAGAC AACTCTGTACAGCACAACCAGCTATCTCAGAGTCAATGAGAGTGAGTGGAAGAGTGAAGAAGTA ACATTCACTTGCGTGTTTGAGAACAAAGCTGGAAATGTGAGGAGAACTGTGGGCTACACTTCATC AGATGGTCCAGTCCATGGACATTCAGTAGTCATTACGATCATCGAGCCGTCTCTTGAGGATATGCT TATGAACAAAAAAGCGCAGCTTGTGTGTGATGTCAATGAACTAGTTCCTGGCTTCCTGAGCGTCA AATGGGAAAATGACAATGGAAAGACCTTAACCAGCCGAAAGGGTGTCACTGACAAAATTGCCAT ACTTGACATCACTTATGAGGACTGGAGCAATGGGACAGTATTCTACTGCGCTGTAGATCACATGG

		AAAACCTGGGGGACTTGGTAAAGAAAGCCTACAAGAGGGAGACCGGAGGAGTTCCACAGCGTCC ATCTGTCTTTCTGCTGGCTCCAGCAGAACAAACTAGTGATAATACGGTGACCCTGACTTGGTACGT CAAAGATTTCTACCCCAAGGACGTTTTAGTGGCTTGGCTTGTTGACGATGAGCCGGTGGAGAGAA CGAGCAGTTCAGCATTGTACCAATTCAACACCACTAGCCAGATTCAATCAGGAAGGACNTACTCT GTCTACAGTCAGCTCACATTTAGCAATGACTTGTGGAAGAACGAAGAAGTGGTCTATAGCTGTGT AGTTTACCACGAAAGCATGATCAAGTCCACAAAAATTCTTATGAGAACCATTGACAGAACCTCAA ACCAACCCAACCTAGTTAACCTCAGCTTGAATGTGCCTCAGAGATGCATAATCACTAGTGAATTC GCGGCC

5

10